The International Journal of Advanced Manufacturing Technology (2018) 97:2255–2292
https://doi.org/10.1007/s00170-018-1973-2

ORIGINAL ARTICLE

Machining of biocompatible materials: a review

Kushendarsyah Saptaji[1] · Mebrahitom Asmelash Gebremariam[1] · Mohd Azmir Bin Mohd Azhari[1]

Received: 11 September 2017 / Accepted: 2 April 2018 / Published online: 10 May 2018

Abstract

The need for more effective and efficient manufacturing processes to transform the biocompatible materials into high standard artificial human body components (implants) is rapidly growing. Machining of biocompatible materials as one of the key processes in manufacturing of implants need to be improved due to the significant effects of machined surface quality to the compatibility and osseointegration with human organs such as tissues, bones, and environment of the human body. The challenges of machining biocompatible materials due to their applications as bio-implants in the human body and the nature of materials properties and microstructures have been explored and solved by various researchers. This article reviews the trends and developments of the machining of biocompatible materials. A range of possible machining technologies and strategies on various biocompatible materials using conventional (milling, turning and drilling) and non-conventional or advanced (abrasive water jet machining (AWJM), ultrasonic machining (USM), ion beam machining (IBM), laser beam machining (LBM), electrical discharge machining (EDM), and electron beam machining (EBM)) are presented and discussed. This review also examines the emerging new technologies such as additives manufacturing and hybrid processes as potential solutions and future research trends in order to fulfill the high standard requirements for a wider range of applications of the biomaterials.

Keywords Biocompatible materials · Machining · Machinability · Conventional machining · Advanced machining · Micro-scale machining · Finite element analysis · Additive manufacturing

1 Introduction

The demand for biomedical implants is rapidly growing in order to improve the quality of human life. The bio-implants are mainly the bio-mimicry of natural and artificial biomaterials used for body components. Such artificial components (implants) can be used for a short period of time, long-term, or even permanent in the biological tissue if not removed surgically [1]. Currently, implants are being used in many different parts of the body for various applications such as orthopedics, pacemakers, cardiovascular stents, neural prosthetics, or drug delivery system [2, 3]. The biomedical components such as shown in Fig. 1 generally must have good corrosion resistance, suitable surface properties, sufficient mechanical strength, biocompatibility with tissues and bones, naturally degraded and disappeared in tissue, and also reliable chemical stability and safety [4]. The materials selections and design have significant effects on the implant lifespan [3].

In this case, metallic alloys such as stainless steel, titanium and its alloys, cobalt–chromium alloys, nickel–titanium shape memory alloys, and magnesium alloys are the most preferable biomaterials. Though ceramics and polymers can also be used as an implants such as in the artificial hip joints [5]. In general, the ceramic and polymer implants are used individually or assembled with other metallic materials. Titanium and its alloys are widely used in joints replacement, spine and trauma systems, dental implants, and pacemaker casings. Magnesium and its alloys are also potential metallic materials to be used as a degradable implant materials because it is less expensive [4]. It is known that magnesium is an essential element of the human body and naturally found in bone tissues and harmless excreted in the urine. However, magnesium is known for its low corrosion resistance especially in saline media that is an environment of the human body. In order to alter the corrosion resistance, surface and subsurface qualities of machined magnesium alloys are normally improved using additional finishing processes such as electrical discharge machining (EDM), electrical chemical machining (ECM), and deep rolling [6].

✉ Kushendarsyah Saptaji
kushendarsyah@ump.edu.my

[1] Faculty of Manufacturing Engineering, Universiti Malaysia Pahang, Pekan, Pahang, Malaysia

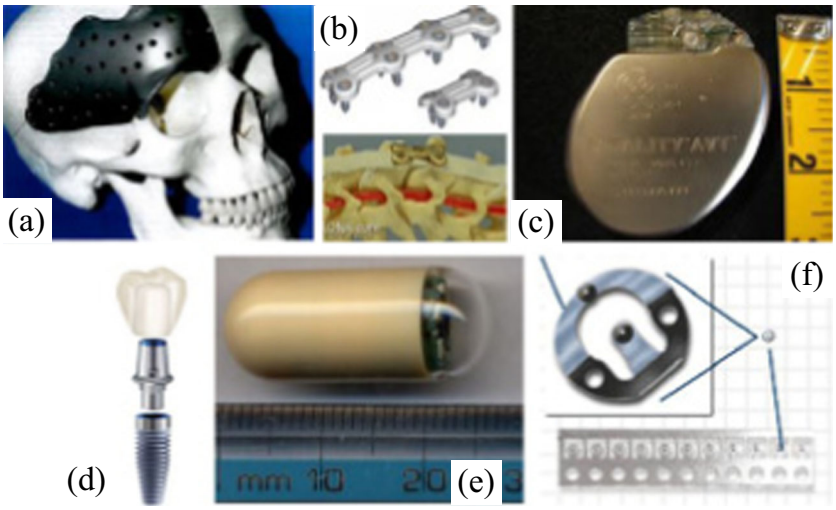

Fig. 1 Sample implant components used in biomedical devices: **a** titanium scaffold, **b** bracket and screws, **c** pacemaker, **d** dental implant, **e** capsule endoscope, and **f** electrical connector in a hearing aid [1]

Alternatively, amorphous alloys or bulk metallic glass (BMG) can also be used as implants [7, 8]. The advantages of BMGs compared with conventional crystalline metals and alloys include high tensile strength, reasonable toughness, high elasticity, low internal friction, excellent wear, and corrosion resistance. These superior properties are attributed to the lack of grain boundaries and crystal defects that usually weaken the material strength, induced intergranular corrosion, and stress-corrosion cracking in biological environments [9]. However, the absence of crystallinity resulted in difficulties in producing and machining of BMG.

Machining of the biocompatible materials as one of the processes in manufacturing of implants (bio-fabrication) has significant impact to the quality of implants. The machining results especially the surface quality will affect compatibility and osseointegration of the implants with human organs such as tissues, bones, and environment of the human body. One of the most demanded bio-implant products in orthopedics that involved machining in its fabrication process is the artificial hip joints or hip joints prosthesis (Fig. 2). Total hip joint replacement is a common orthopedic surgery today in order to increase life expectancy and to support a more active lifestyle. The hip joint prosthesis is used to reduce the pain and immobility of the arthritic patients. The most important part in hip joint prosthesis is the femoral head that has spherical shape. Additional finishing process such as grinding or polishing of the femoral head must be conducted in order to achieve the required surface quality. The femoral head needs to have properties such as low surface roughness, good friction resistance, high wear resistance, good corrosion resistant, and high mechanical strength due to the bearing mechanism and the various movements. More importantly, it also must have a good biocompatibility to avoid inflammation and rejection [4].

Therefore, the concern in machining of bio-implant materials is mainly the surface and subsurface quality of the machining results such as surface roughness and residual stress. The surface quality will affect the mechanical performance of implants. Two common issues related with the surface quality are corrosion resistance and wear resistance. Corrosion and wear can cause a decrease of the biological compatibility and can lead to bio-implants malfunction. Hence, the intention of this paper is to review some efforts from researchers on the attempts to solve some challenges related with machining of biocompatible materials and some development in the new methods to improve the machining processes and the quality of machined biocompatible materials.

This paper focuses mainly on the machining of metallic biocompatible materials with few discussions on ceramics, polymers, and living materials such as bones. The discussion will be emphasized on three machining methods: conventional, non-conventional (advanced), and other processes that are currently being studied such as in microscale machining, simulations and modeling of machining biomaterials, advanced multi-axis machining processes, additive manufacturing, and hybrid process. The machinability performance, surface roughness, and other machining characteristics of biomaterials will be discussed with respect to the different machining strategies.

The machining of biocompatible materials using conventional methods including milling, turning, and drilling processes are detailed in "Conventional machining of biocompatible materials"section where the mechanisms of material removal as the effect of cutting parameters, tool materials and cutting forces on the surface roughness, micro-hardness, microstructure, and other properties are further discussed. The "Non-conventional machining of biocompatible materials" section specifically reviews the nonconventional or advanced machining processes (abrasive water jet machining (AWJM), ultrasonic machining (USM), ion beam machining (IBM), laser beam

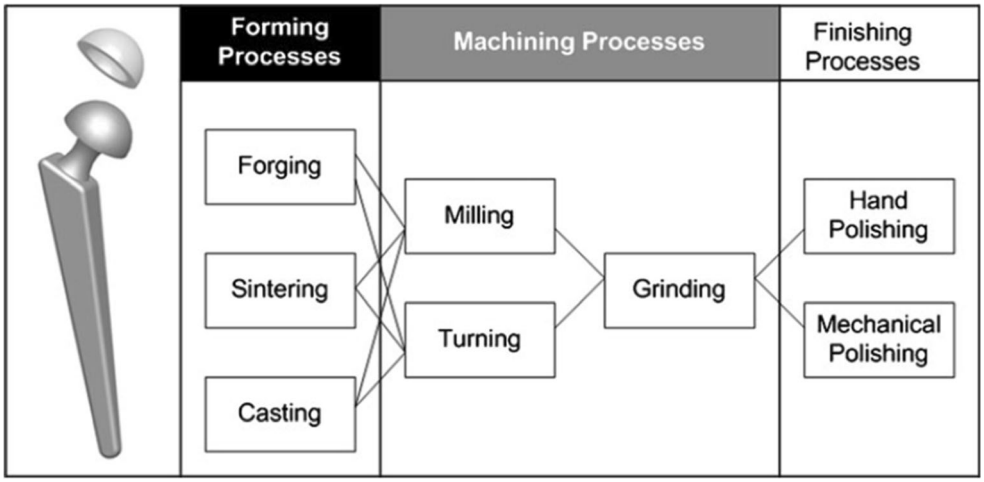

Fig. 2 Fabrication process plan for metallic components of prosthesis [10]

machining, electro discharge machining (EDM), and electron beam machining (EBM)) of the biomaterials including metals, ceramics, polymers, and composites where the main characteristics of machining results are discussed in detail. In "Current status and future trends of machining of biocompatible materials" section, a review of the state of the art research, current, and future trends of machining biocompatible materials is proposed in order to solve the challenges of miniaturization, complex shape, tighter accuracy, and tailored surface roughness of implants. It is dedicated more on micro-scale machining, simulations and modeling to predict the machining performance, CNC multi-axis machining strategies, additive manufacturing, and hybrid machining processes. It is expected that improvements and optimization of the various machining processes of biocompatible materials discussed at length in this paper can be articulated and used by the researchers and industries involved in the manufacturing of artificial human body components.

2 Conventional machining of biocompatible materials

This section discusses some research results on the conventional machining processes of biocompatible materials that can be implemented in one of the steps in the implants fabrication. Some of the implants that may involve conventional machining are artificial heart valves, artificial ligaments, prostheses in dentistry, dental implants, hip implants, screws, connecting parts, small bone plates, vertebrae implants, bone screws, bone plates, surgical instruments, prosthetic components, and special implants. Though the production of such products is not direct machining process, it normally will through this route: design such as computer-aided design–computer-aided manufacturing (CAD-CAM)—Computer Numerical Control (CNC) machining which normally uses five-axis multitasking CNC machine. Alternatively, other route such as CAD-RP-RT-IC (rapid prototyping, rapid tooling and investment casting (IC)) have lesser cost compared to the previous route in the case of stainless steel femoral stem in hip prosthesis fabrication [11].

The term conventional machining process is referred to milling, turning, and drilling processes. These processes are usually performed in the earlier step of the machining processes (roughing machining) of bio-implants. In the recent technology of implants manufacturing where the additive manufacturing (AM) process is used, machining is still needed as post-processing process in order to achieve the required surface quality and to achieve the desired shape. One of the implants that involved conventional machining process during their fabrications is femoral stem in hip prosthesis [11].

In this section, discussion will be mainly on the research on machining of biocompatible materials which some of the references are indirectly related with the fabrication of the implants. The discussion are mainly on the metallic alloys especially magnesium alloys (AZ31 and AZ91 series), titanium alloys (Ti-6Al-4V), bulk metallic glass (BMG Zr-based), shape memory alloys (SMA) NiTi, and very few on polymers. Table 1 presents the summary of the application of these biocompatible metallic alloys due to their advantages and the challenges when using conventional machining and the proposed solutions to overcome the challenges. The concerns from conventional machining process point of view are mainly on the selection of suitable machining process and machining parameters such as feed rate, cutting speed, depth of cut, machinability of the biocompatible materials, additional coolant, and tool materials. These, at the end, not only affect the surface and subsurface properties but also tool wear conditions and efficacy of the machining process.

In the machining of high strength magnesium alloys such as AZ31 and AZ91 series, the surface needs to be smooth while the subsurface properties in the form of residual stress needs to be favorable. The machined surface also needs to

Table 1 Comparison of main advantages and disadvantages during machining of biocompatible metals using conventional machining processes

Materials	Application as implants	Advantages as implants	Disadvantages in the conventional machining process	Solutions
Magnesium alloys	Cardiovascular stent [12]	Essential element of human body	Flame ignition	Lower cutting speed and lower depth of cut [13]
	Orthopedic implants [14]	Naturally found in bone tissues	Flank built-up (FB)	Deep rolling process [6]
	Screw	Harmless excreted in urine	Low corrosion resistance	Hybrid machining-burnishing process
Titanium alloys	Spherical prosthesis [10]	High biocompatibility	Variation in chip thickness	Thermally enhanced machining
	Dental screws	Specific strength	Heat stress	Cryogenic coolant [15–17]
	Hip replacement	Corrosion	Pressure load	High conductive cutting tool
		resistance [18]	Spring back Residual stress	Coated carbide tool
Shape memory alloys NiTi	Osteosynthetic plate [19] Bone plates [20]	Alter the stiffness of the implants at a particular time	High tool wear	High cutting speed and feed
		Improve the bone healing process in terms of healing time	Adverse chip formation Burrs formation	Cryogenic coolant [16]
		Stability [19]		
		Excellent fatigue properties at high strain levels [20]		
Bulk metallic glass	Dental implants Stents Orthopedic surgeries	High tensile strength High toughness High elasticity	Light emission Tool wear	Low cutting speed [21]
	Sutures [8]	Low internal friction		
		Excellent wear		
		Good corrosion resistance		

have good corrosion resistance when it is being used as bio-implants [6]. The issues in machining magnesium alloys are the flame ignition and flank built-up (FBU) especially at higher cutting speeds. The flame ignition occurs due to the high temperature during the cutting process and relates with the safety considerations during machining process, whereas the FBU occurs due to the adhesion of workpiece material to cutting tool, which in the end produces unsteady machining forces with an inferior surface quality [22]. Therefore, the parameters for machining process and the tool materials have to be properly controlled. The FBU can be avoided by using lower cutting speed and depth of cut [13], while the corrosion resistance can be improved by additional finishing processes such as deep rolling [6].

The common problems in machining of titanium alloys are variations in chip thickness (serrated chip), heat stress, pressure load, spring back, and residual stress. These problems and its proposed solutions such as thermally enhanced machining, use of cryogenic coolant, use of high conductive cutting tools such as diamond tool, and hybrid machining have been extensively discussed by Pramanik [23] and Gao et al. [24]. Similar challenges faced in machining SMA NiTi are high tool wear, adverse chip formation, and burrs formation [25]. Shape memory alloys NiTi are also known for difficult to machine materials due to its high ductility, high degree of strain hardening, and unconventional stress–strain behavior [26]. One of the methods to improve the machining results is by optimizing the machining parameters such as high cutting speed and feed.

The cutting parameters used in the machining process such as milling, turning, and orthogonal cutting are also important not only on surface integrity but also tool wear. In the case of machining titanium alloys, tool wear problem is the main concern. Besides affecting the tool life, tool wear will also affect the surface integrity of machined titanium alloys, which is important as implants. The chip formation analysis can be used to analyze the tool wear and the surface quality. The saw tooth and serrated shape of chips are typically formed in the machining of titanium alloys. The formation of this chip shape is mainly due to the catastrophic thermoplastic shear model. It was reported that the degree of serration is more pronounced and evident as cutting speed, feed, and depth of cut increase [27].

In most of the experimental results, cutting speed is the main factor in surface quality and tool wear compared to feed rate and depth of cut. Some researchers [15–17] have applied cryogenic type of machining in order to extent the tool life. The application of cryogenic coolants can prevent heating up

between the tool cutter and the biomaterial by pouring cryogenic coolants such as liquid helium, air, liquid nitrogen (LN_2), and liquid carbon dioxide (LCO_2) in the cutting zone. The machining temperature can go down to −150 °C so that chemical reactions, adhesion, and diffusion of the tool can be minimized; hence, the tool life would be extended. Besides the applications of cryogenic coolant, the tool wear can also be minimized by using coated carbide tools [28]. In addition to the surface quality and the tool wear, the fatigue resistance is also important in machining biocompatible titanium alloys [29].

In the machining of BMG, the main concerns and observations are in the light emission and the tool wear occurred at higher cutting speed. It has been reported that forces in machining BMG are in between stainless steel and aluminum in turning process and micro-milling process [30, 31]. One of the characteristics in machining of BMG is that no preference orientation occurred during chip formation due to the nature of their microstructure. Hence, the chips separation is mainly by shear banding behavior resulted the chips to be torn off along a shear plane [32].

2.1 Milling

Milling process is a versatile metal cutting process and considered as an oblique cutting process where the cutting edge is not perpendicular to the cutting velocity. Cutting action in the milling process is performed by single or multi cutters (flutes) in rotational motion [33]. In the machining of biocompatible materials, optimization of milling parameters such as cutting speed, depth of cut, and feed rate are very essential to increase productivity of the process and to improve the machined workpieces quality.

Milling process has been used as part of the artificial limb fabrication [34]. In order to fabricate artificial limb, the process flow from the 3D data acquisition, CAD, CAM, and CNC milling using three-axis CNC milling machine using polyurethane resin as the workpiece was reported. Two steps CNC milling process was conducted. The roughing is conducted using end milling while the finishing was conducted using ball end mill. In general, the fabrication of implants such as artificial limb, hip prostheses, and residuum for lower limb amputee follows conventional procedure using reverse engineering method. The reverse engineering method is suitable especially for personalized implants. A 3D scanning is used to scan the normal or original organ body. Subsequently, the 3D scanned data is adjusted using CAD system. After that, CAM is used to design tool paths, optimal process conditions, and tools in order to get rapid production of the implants using CNC machine. Next, machining is conducted using three-axis CNC machine or five-axis multitasking CNC machine. The five-axis multitasking CNC machine is more favorable since the implants normally have complex shapes so that the combination of milling and turning as well as the five-axis motion can achieve the intended quality. However, three-axis CNC machine can also be used which normally only the milling process is involved.

Reverse engineering method is also reported when fabricating personalized residuum liner for lower limb amputee [35]. In order to produce the personalized residuum, the plaster cast is made from the patient residuum, followed by scanning to get the digital model. This will enable seamless and fluid capture of a person's specific anatomical data and can be carried out using analogue or digital methods. The digital model is then modified and refined in the CAD process. Subsequently, the process plan is created using CAM. The implant is made of soft polymer neoprene foam. Cryogenic machining in CNC machine using 8-mm ball nose is conducted below the glass transition temperature (Tg) of neoprene foam in order to harden the neoprene foam.

Shi et al. [36] studied the optimum milling parameters of AZ91D series magnesium alloys using grey relational analysis and Taguchi L9 (3^3) orthogonal array method. The milling experiments were conducted using uncoated fine-grained carbide grade inserts with a diameter of 20 mm and in dry conditions. It was observed that feed rate was the more significant factor compared to cutting speed and depth of cut in affecting surface roughness and micro-hardness in milling of AZ91D alloy. The temperature rise during machining process of magnesium alloys also needs to be controlled in order to avoid the inflammation. The low temperature can be achieved by decreasing the cutting speed and the depth of cut [13]. Kuczmaszewski et al. [13] reported an overview of the state of knowledge on temperature measurement in the cutting area during milling of magnesium alloys AZ31 and AZ91 series. The milling experiments were conducted using a 16-mm TiAlN-coated carbide end mill and fixed radial depth of cut of 14 mm. The cutting parameters used were axial depth of cut ranged from 0.5 to 6 mm; feed per tooth 0.05, 0.15 and 0.3 mm/tooth; and cutting speed 400, 800, and 1200 m/min. The temperatures during milling were measured using infrared images. They argued that cutting speed and feed rate modifications are seen not to induce significant temperature growth and maximum temperature in the cutting area. No inflammation was observed during the experiments due to the low measured chip temperature in the cutting area compared to the temperature needed for chip ignition or the melting point of magnesium alloys.

In order to improve the corrosion resistance of biodegradable magnesium–calcium (MgCa) alloys, Salahshoor et al. [37] proposed a hybrid dry cutting-finish burnishing process. The experimental setup for high-speed milling and burnishing is shown in Fig. 3. The Mg–Ca alloys workpiece is milled using polycrystalline diamond (PCD) inserts in high-speed milling machine. The experimental work and finite element simulation were conducted in order to investigate the effect of

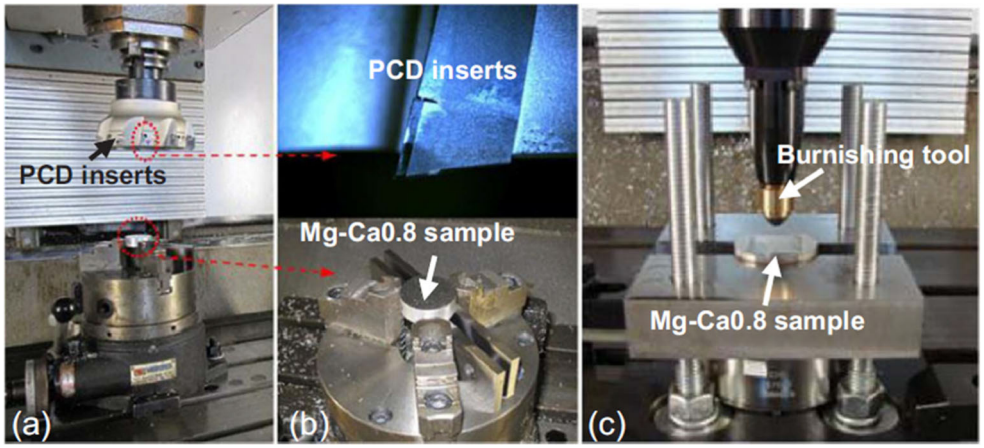

Fig. 3 Experimental setup of the hybrid cutting-burnishing process: **a** high-speed milling setup, **b** MgCa0.8 sample in milling and PCD inserts, and **c** burnishing setup [37]

milling speed and rolling force. Experimental work shows that surface roughness (R_a) of the burnished surfaces are higher than milled surfaces. However, the residual stress especially in the subsurface is more compressive for the burnished surfaces compared to the milled surfaces. In the end, the milled surfaces are more susceptible to corrosion compared to burnished workpieces.

The effects of cutting parameters especially cutting speed on cutting forces, tool wear, and surface integrity (surface roughness, micro-hardness, and microstructure beneath the machined surface) in the high-speed milling of alpha-beta titanium alloy Ti-6Al-4V have been studied by Wang et al. [38]. The experiments were conducted using cemented Ti (C, N)-Al_2O_3-coated carbide cutting tools with cutter holder diameter of 25 mm, using dry milling and down cutting. The cutting speeds selected in the experiment ranged from 100 to 400 m/min; the feed per tooth were 0.05 and 0.10 mm; and the radial depths of cut were 0.5 and 1.0 mm. The axial depth of cut was kept constant at 5.0 mm. The experimental results show the trend that cutting forces in all three directions increase with cutting speed, feed per tooth, and depth of cut. The low cutting forces and improved surface roughness were obtained at cutting speed of 200 m/min for different depth of cut as shown in Fig. 4. The widths of flank wear were seen to increase rapidly with the increasing cutting speed and the tool wear was the main effect in cutting forces variations at higher cutting speed. In terms of microstructure on the subsurface, the grains at near-surface were slightly elongated in the feed direction when cutting speed 400 m/min and feed per tooth 0.10 mm. The hardness of machined surface was observed to be decreased with the increase of cutting speed and feed per tooth due to thermal softening effect.

Most of the implants made from biomaterials have complex shape and freeform surface such as the femoral head implants. Therefore, the machining of spherical surface is indeed necessary to be studied, especially the factors affecting process and surface quality. In order to improve surface quality and to avoid smeared/adhered material of the freeform surface when machining Ti-6Al-4V using four-axis machining center, the effect of lead and tilt angles between the tool axis and the surface normal vector in four-axis machining center are analyzed [39]. The surface roughness on the flat surface

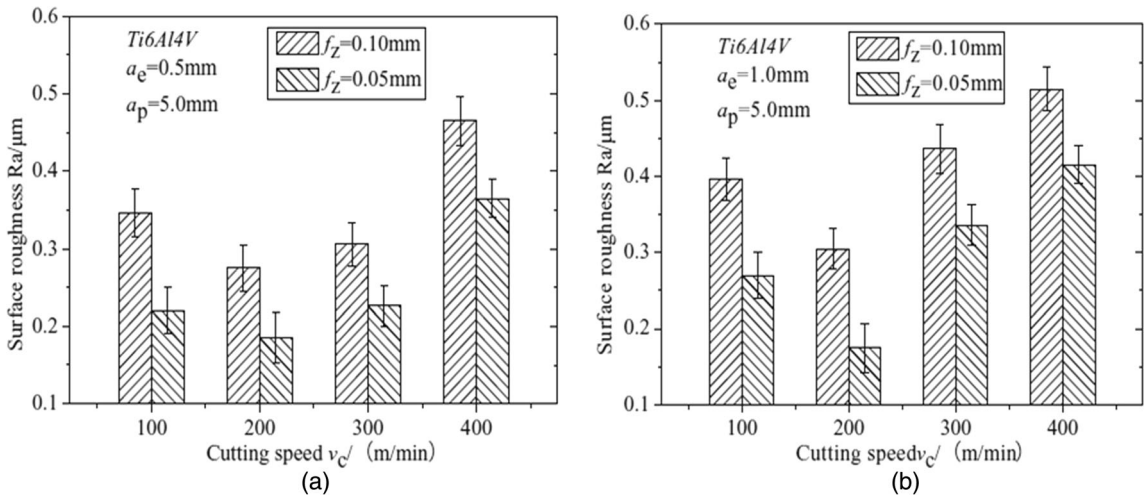

Fig. 4 The surface roughness of the milled surface at different cutting parameters **a** radial depth of cut 0.5 mm and **b** radial depth of cut 1 mm [38]

is homogeneous, whereas a non-homogenous roughness is seen on the concave and convex surfaces (Fig. 5). It was found that tilt angle has a strong effect on the quality of the titanium alloy surfaces, with the best quality surfaces were obtained using the greatest positive tilt angles (oblique-reverse-push-up milling).

The effect of cutting angles (axial and radial rake angle) on surface integrity (roughness and the residual stresses) and fatigue properties in the milling Ti-6Al-4V have been studied [29]. It was reported that the fatigue limit is sensitive to the surface integrity [29]. In this study, the edge radius was chosen to be constant in order to focus only on the effect of cutting angles on roughness and residual stresses. The cutting parameters used were cutting speed of 50 m/min; a feed per tooth of 0.3 mm/tooth; an axial depth of cut of 1 mm; and a radial depth of cut of 100%. As a result, the flank wear remained nearly constant 0.05 mm ± 0.02 mm, the edge radius remained also nearly constant 26 μm ± 3 μm, and the first notch on the cutting edge occurred at 11 min. The results showed that the cutting angles have a less effect on surface roughness parameters, but greater effect on residual stresses. It is argued that a negative axial rake angle induced compressive residual stresses regardless of the radial rake angle. In contrast, a positive axial rake angle combined with negative radial rake angle induced tensile residual stresses and a higher edge radius increased size of the layer affected by machining.

2.2 Turning

Turning is typically applied to machine a cylindrical part where the tool is fixed while the workpiece is rotated. Study on the turning of biocompatible materials is focused on the effects of turning parameters such as depth of cutting, feed rate, spindle rate, and additional coolant to improve the surface quality of machined surface and tool life. Denkena and Lucas [6] reported comparison of the subsurface properties (residual stress) and the effect of corrosion resistance of magnesium alloys produced by turning and deep rolling. In order to achieve comparable low surface roughness, the parameters of both processes were controlled. The measured residual stresses showed that the highest compressive residual stress is in a depth of about 160 μm in the turned specimen with a cutting speed of 10 m/min. In addition, it was observed that subsurface properties and corrosion progression have strong correlation after the workpieces were tested by corrosive mass loss method using 0.9 wt% *NaCl* saline medium. It shows that

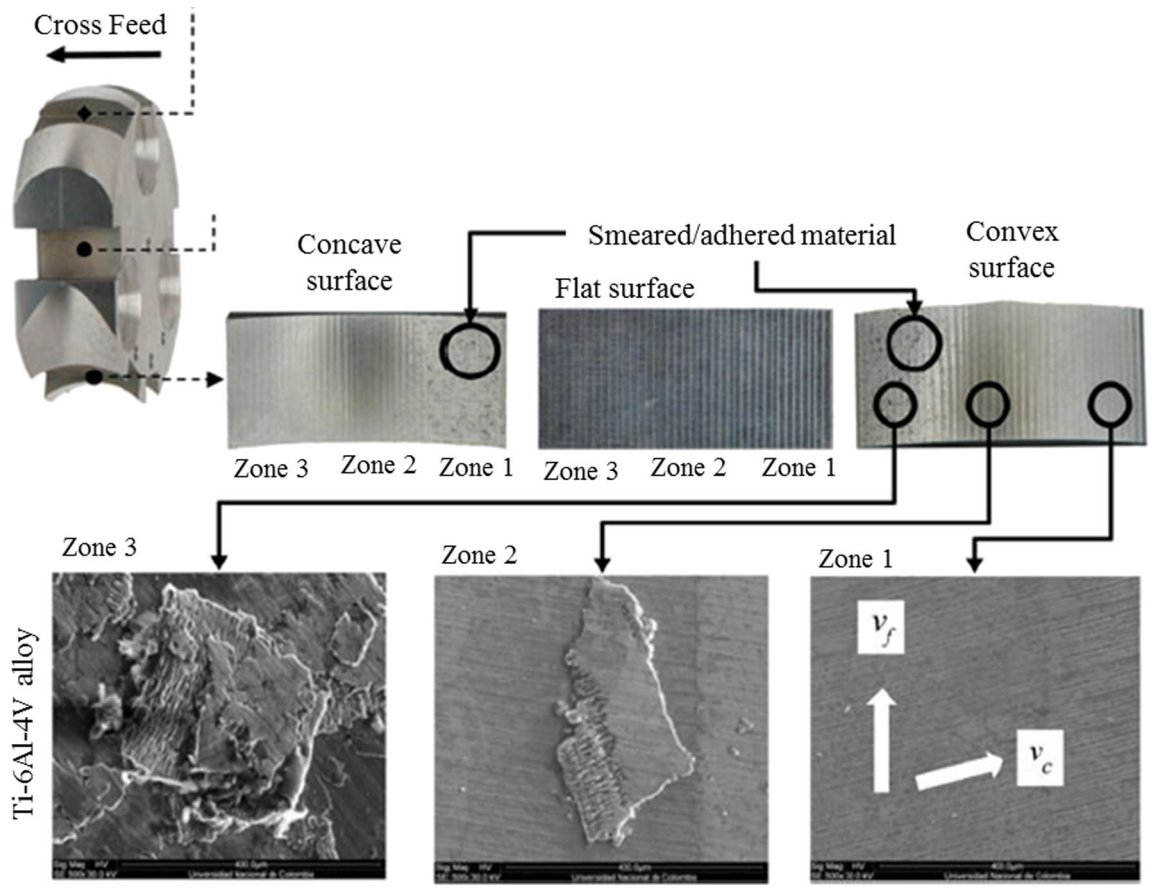

Fig. 5 Samples of the machined surfaces (inclination lead angle = − 25°). Scanning electron microscope images of three areas of the concave surface of Ti-6Al-4V alloy (500×) [39]

the deep rolling process can successfully reduce the corrosion rate of magnesium alloys by a factor of approximately 100 due to high residual compressive stresses generated in the subsurface.

Sun et al. [15] investigated the effect of cryogenic compressed air cooling on the development of tool wear and the evolution of cutting forces in turning Ti-6Al-4V alloy at two different cutting speeds. Turning was conducted with a carbide insert having a rake angle of +15°, an entry angle of 45°, an inclination of −6°, and an effective rake angle of +9°. Cutting was performed at cutting speeds of 150 and 220 m/min with constant depth of cut 1 mm and feed 0.28 mm. The cryogenic compressed air jet was applied in the flank face and the rake face of the tool during machining. The cryogenic compressed air was generated by passing the compressed air at a pressure of 7 bar and was cooled to the temperature of −196 °C. The cutting was interrupted with every 5.2 cm^3 of material removed. In order to measure the temperature, the emissivity of the workpiece alloy was calculated by calibrating the temperature reading from infrared signal with the temperature measured by thermocouples. It was found that the chip temperature increases with an increase of flank wear width because of the increase in coefficient of friction. At the beginning of cut, cutting forces with the application of cryogenic compressed air cooling are higher than those under dry machining, but are lower with an increase in accumulative cutting time. The cutting forces reduction when using cryogenic compressed air cooling is more significant at higher cutting speed because of the significant reduction in size of chip built-up edge. The flank wear width is significantly reduced with the application of cryogenic compressed air cooling, which can be attributed to the smaller recession of the cutting edge due to effective cooling in cutting zone [15].

Sutter and List [40] studied the high-speed orthogonal cutting of Ti-6Al-4V alloy with large depth of cut (0.1–0.25 mm) in order to analyze the dynamics and evolution of the chip geometry. Two different setups were prepared. First setup was prepared on NC Lathe to cover the cutting speed from 300 to 1200 m/min. The second setup was prepared on specific ballistic setup to cover the cutting speed from 300 to 4400 m/min (Fig. 6). The tool used was uncoated carbide tools. The cutting speed was observed as the main factor in determining chip morphologies. At the speed of 45 m/s for depth of cut of 0.1 mm and at the speed of 20 m/s for depth of cut of 0.25 mm, the chips were seen to be severely deformed resulting in the discontinuous chips. Based on their observations, the evolution of chip morphologies as the effect of cutting speed can be classified as (Fig. 7): (1) the regular serrated chip formation, (2) the serrated chip formation with transition involving a compression phase of the segments, and (3) the formation of discontinuous chips.

It is reported that in the orthogonal cutting of Ti-6Al-4V using polycrystalline diamond (PCD) tool, the application of cryogenic method reduced the cutting force of about 25% compared to ambient dry cutting conditions [17]. Furthermore, the additional of 10% ethanol in the metal removal fluid (MRF) using flooded machining method reduced the cutting force down to 65% and produced lower surface roughness. The application of cryogenic coolant resulted in separated chip segments compared to serrated attached chip segments under ambient dry cutting (Fig. 8). This shape is similar to the chip characteristics produced at high cutting speed [40].

Abellan et al. [10] have made comprehensive analysis on the contour error, the effect of cutting parameters on surface roughness, the effect of coordinate measuring machine (CMM) on sphericity error, and the effect of sensor measurements related with the turning of Ti-6Al-4V and Cr–Co spherical features when using uncoated tungsten carbide tool. The equipment and setup used in their experiments are shown in Fig. 9. The analysis was conducted as part of the fabrication process of spherical prostheses implants. It was reported that the contour error needs to be always lower than 9 μm for any cutting conditions in order to achieve the optimum spherical

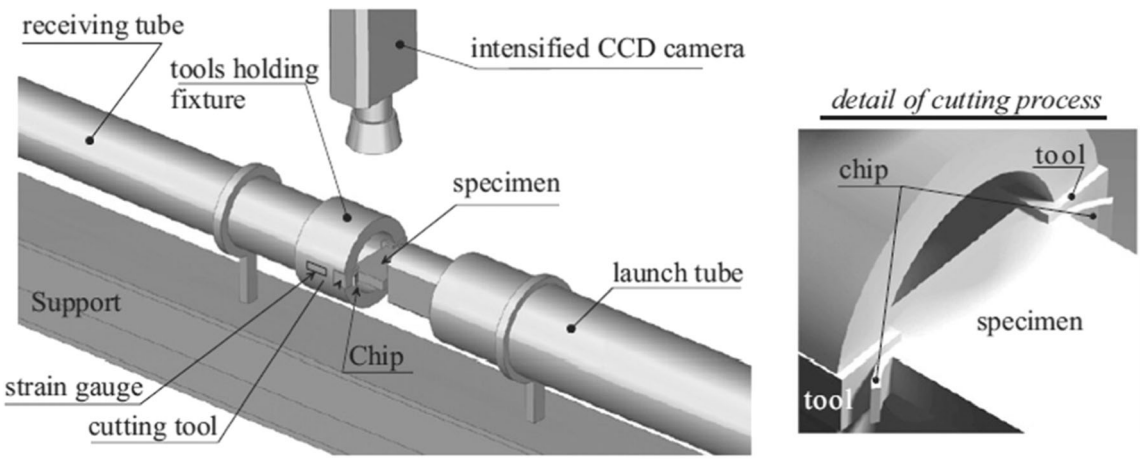

Fig. 6 Ballistic cutting setup for high cutting experiment [40]

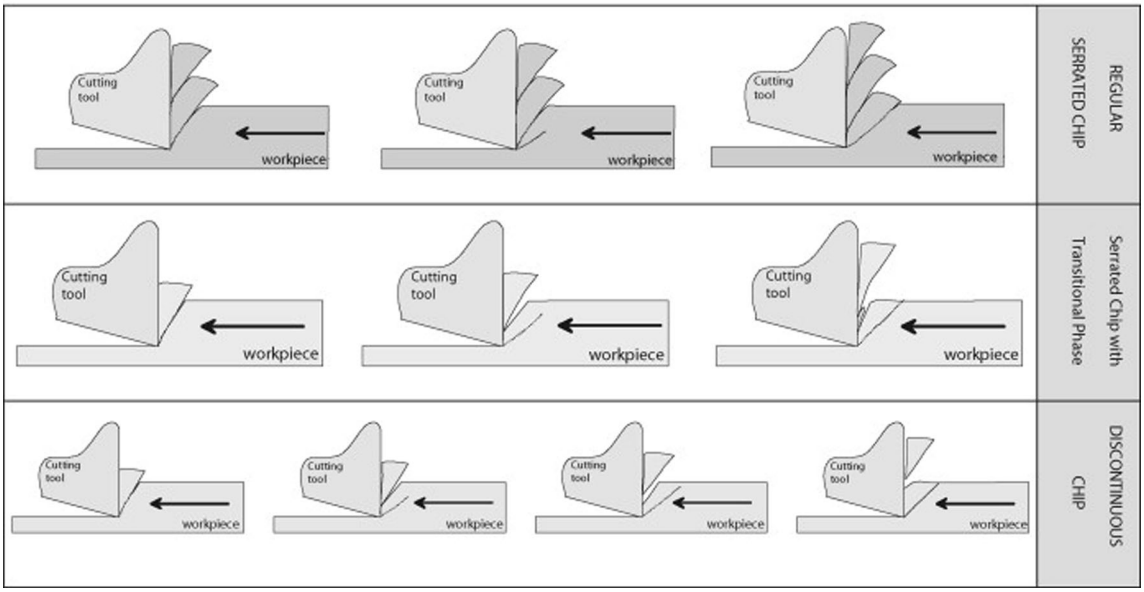

Fig. 7 Schematic sequences of chips formation in Ti-6Al-4V machining for high cutting speed [40]

shape. The comparison between the experimental results shows that the machined Ti-6Al-4V has lower surface roughness value compared to Cr–Co. The results also show that sphericity error in the measurement using CMM was related with the number of measurement points.

NiTi shape memory alloys (SMA) is also well known as difficult-to-machine materials that can be used as bio-implants due to their unique properties [16]. The high tool wear is also the main concern in the machining of NiTi shape memory alloys (SMAs) similar to the machining titanium alloys. Kaynak et al. [16] conducted experimental work on turning of NiTi to understand the interrelationships between tool wear mechanisms, patterns of progressive tool wear, and chip formation during machining of NiTi alloys, with the final objective to develop predictive performance models for the tool life. The cutting experiments were conducted using a constant feed rate and depth of cut: 0.05 mm/rev and 0.5 mm, respectively. In the first series of experiments, investigation on the effects of cutting speed on tool wear rate was conducted. The cutting speed was varied at 12.5, 25, 50, and 100 m/min with a constant cutting length of 26 mm. In the second series of experiments, a progressive tool wear test was carried out at constant cutting speed of 25 m/min. They observed that the minimum quantity lubricant (MQL) method was not effective in reducing tool wear at high cutting speeds and a flow rate of 60 ml/h, which is a typical condition used in machining of NiTi alloys. In contrast, the cryogenic cooling is effective in reducing the tool wear rate at higher cutting speeds. Furthermore, progressive flank wear is reduced at the nose region and notch wear at the depth of cut line at lower cutting speeds during machining of NiTi shape memory alloys as shown in Fig. 10.

Bakkal et al. [21] conducted turning experiments on $Zr_{52.5}Ti_5Cu_{17.9}Ni_{14.6}Al_{10}$ bulk metallic glass (BMG). The cutting tool used was a TiN-coated WC-Co insert having a 0.4-mm tip radius and a 5° rake angle. All tests were conducted in dry condition using constant feed per revolution and depth of cut at 0.025 mm/rev and 0.5 mm, respectively. The constant depth of cut and feed per revolution were used in order to get the same uncut chip profile for all cutting speeds. Three cutting speeds, 0.38, 0.76, and 1.52 m/s were used. It was found that there is no macroscopic plastic strain occurred which is

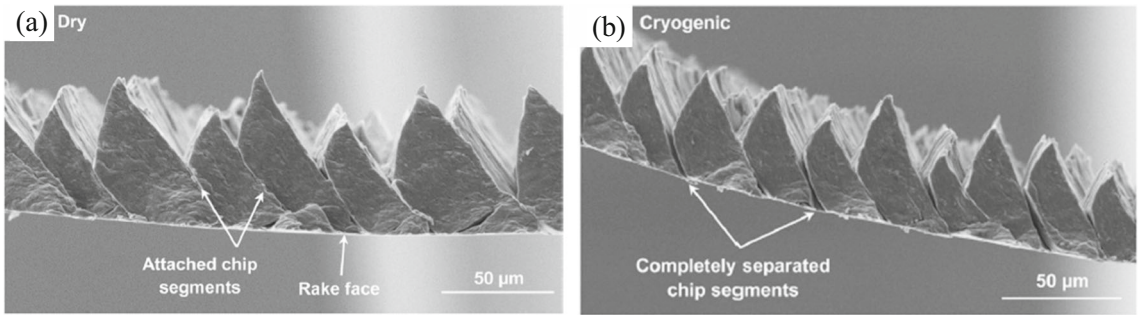

Fig. 8 SEM images of serrated chip formation in the orthogonal cutting of Ti-6Al-4V: **a** under ambient dry cutting conditions and **b** under pre-cooled cryogenic cutting conditions [17]

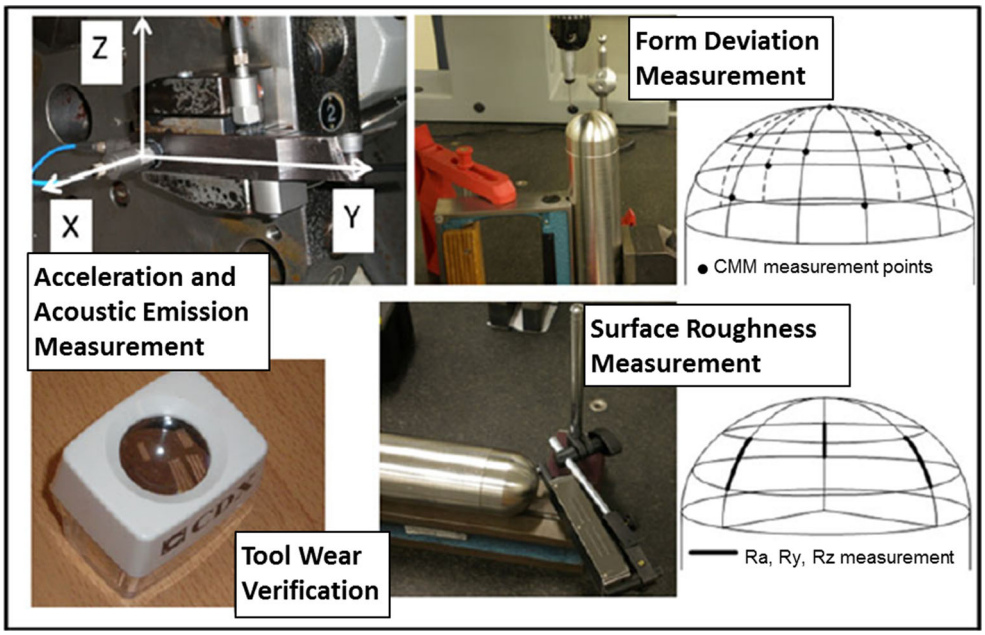

Fig. 9 Equipment and setup for offline and in-process measurements on the contour error, surface roughness, sphericity error, and tool wear [10]

similar in machining of brittle materials. However, BMG produces a continuous ductile chip similar to conventional metal machining. Large shear lamella was observed similar to the serrated chips produced using Ti alloys.

At the two highest cutting speeds, 0.76 and 1.52 m/s, the emission of light was observed in the tool–workpiece contact region (Fig. 11) and a surface layer and interior crystallization were found in the chips. At the highest cutting speed, 1.52 m/s, the chip formation is a combination of irregular lamellar segments in the midsection, surrounded by string-like features resembling "taffy-pulls." In contrast to the chips, the machined surfaces do not undergo crystallization at any of the cutting speeds. It is argued that major portion of the heat generated will flow into the chips due to the very low thermal conductivity of BMG.

Bakkal et al. [30] also reported on the turning study of Zr-based bulk metallic glass ($Zr_{41.2}Ti_{13.8}Cu_{12.5}Ni_{10.0}Be_{22.5}$ BMG) materials. Turning experiments were conducted by using three variables, which are four tools (WC-PVD, WC-CVD, PCBN, and PCD), three cutting speeds (0.38, 0.76, and 1.52 m/s), and three work materials (BMG, Al6061, and SS304). The purposes of their work are mainly to study the process conditions that trigger the light emission and analyze cutting forces, chip morphology, surface roughness, and tool wear in the lathe turning of Zr-based BMG compared to AISI 304 and Al 6061. The depth of cut and feed per revolution were constant which are 0.5 mm and 50 μm/rev in all cutting tests. Similar to the results achieved in [21], at lower cutting speed, the light emission has not occurred. However, the serrated chip with adiabatic shear band and void formation was observed. In contrast, at the higher cutting speeds of 0.76 and 1.52 m/s, light emission was observed due to enough energy delivered to the chip which activated the oxidation. Surface roughness of the machined BMG surfaces is generally better than the other two work materials. In addition, the tool wear is expected to be the main concern for machining of BMG.

In another work [41], the influences of machining parameters (i.e., depth of cutting, feed rate, and spindle rate) on the surface quality and chip morphology of a Zr-based ($Zr_{41.25}Ti_{13.75}Ni_{10}Cu_{12.5}Be_{22.5}$) BMG on the ultraprecision turning experiments were studied. This Zr-based BMG is known to have no iron content hence can avoid diamond graphitization during diamond turning. A single-crystal diamond tool with a nose radius of 0.25 mm was used to cut the

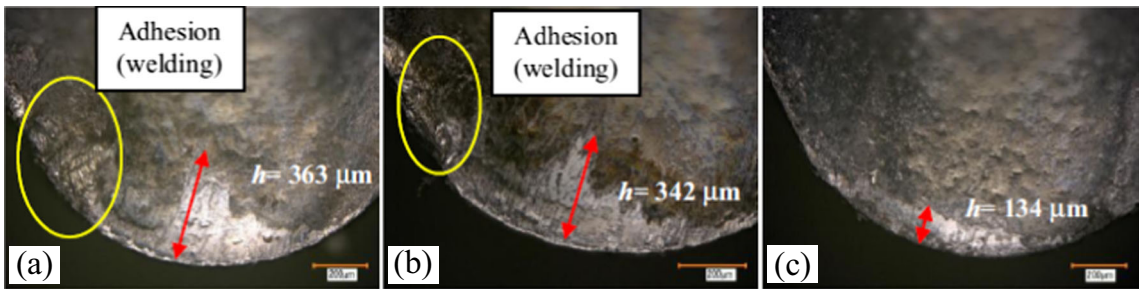

Fig. 10 Tool–chip contact length after 1 min of cutting for **a** dry machining, **b** MQL machining, and **c** cryogenic machining [16]

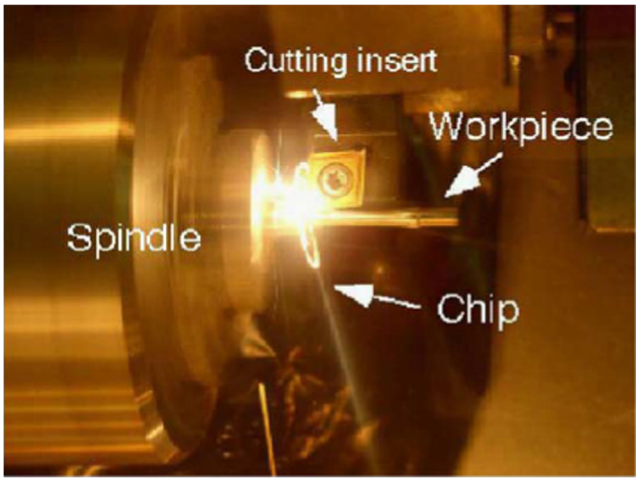

Fig. 11 Light emission from tool–workpiece contact area and chip during turning of Zr-based bulk metallic glass [21]

BMG sample. Two depths of cut of 1 and 3 μm were used in the experiments. Two feed rates of 10 and 20 mm/min and two spindle speeds of 500 and 2000 rpm were used. At larger depth of cut (3 μm), the formation of regular sinusoidal-like grooves was observed. Furthermore, increasing the feed rate produces lower surface roughness, but the processing instability increases, causing irregular grooves to appear on the surface.

2.3 Drilling

Drilling process is generally applied to produce holes in biomaterials parts. The material removal process in drilling occurs as the action of rotation of one or more flutes of the drilling tool. The issues in the drilling process of biocompatible materials are the hole surface quality especially at the edges and the tool breakage. There are not many studies on the drilling process of biocompatible materials found in the literature. However, Sunil et al. [42] reported that the difference in an amount and a distribution of the secondary phase, $Mg_{17}Al_{12}$, in AZ31 and AZ91 magnesium alloys show significant effect in the machining of magnesium alloys especially in the drilling [42]. Drilling experiments were carried out by producing holes with spindle speed 45, 235, and 450 rpm and feed rate 10, 15, and 30 mm/min using 6-mm diameter high-speed steel twist drill bit without using lubricant. Experimental results showed that a lower cutting force was generated during drilling of AZ31 as compared to AZ91 alloy. It is argued that the lower cutting force in drilling AZ31 is due to the presence of uniform α phase. The chips produced in the drilling of AZ91 alloy are seen to be discontinuous due to the combination of soft and brittle regions that belong to α and β phases. In all experiments, no flank built-up (FBU) was observed. This mainly due to the range of drilling parameters used in the experiment is not sufficient to generate the heat.

3 Non-conventional machining of biocompatible materials

Most biomaterials are considered to have a hard and abrasive nature, ordered structures (microstructures), and less stiffness which make them very difficult to machine. The conventional (traditional) machining (shaping) processes could not meet the existing material removal requirement due to the nature of metallurgical microstructure, and hence, there have been recent developments in cutting tool technology applicable to the machining of, for example, the medical graded materials. More importantly, there were several research works of non-conventional or advanced machining processes that have made a breakthrough in the machining of biocompatible materials. These newer processes are called non-conventional or advanced in the sense that they do not employ conventional tools for machining. These non-conventional machining processes of the biocompatible materials have been well expanded and their applicability has satisfactorily suited to various existing and newly developed metals, polymers, ceramics, rubber, and composites. The types of non-conventional machining techniques are many which include abrasive water jet machining (AWJM), ultrasonic machining (USM), and ion beam machining (IBM). There are also other techniques which basically use the principle of chemical and electromechanical processes. These include machining by laser beam machining (LBM), electrical discharge machining (EDM), and electron beam machining (EBM). The applications of various non-conventional machining processes on biocompatible materials are summarized in Table 2. In addition, the complex shapes of the bio-implants are sometimes difficult to be produced by conventional machining; hence, alternative fabrication processes needs to be developed. The advanced machining process needs to be added as a finishing process in order to improve or modify the surface quality of the bio-implants surface produced by conventional machining. In this section, a thorough review on some of the non-conventional machining processes applied on biocompatible materials and their future applicability are discussed.

3.1 Abrasive water jet machining

Abrasive water jet machining (AWJM) is one of the shaping tools that fulfill the ideal requirements of material removal mechanisms for biocompatible materials. This process is mainly used to machine biomaterial samples as well as to improve the surface finish of biocompatible implants. Basically, water is compressed to ultrahigh pressure and released from a very small orifice, thus generating a high-velocity water stream [93]. If abrasive particles are added to the fast flowing water stream, its machining capability can be significantly improved [94]. The illustration of AWJM process is shown in Fig. 12. This technology offers

Table 2 Applications of non-conventional machining processes on biocompatible materials

Process	Materials used	Reference
Abrasive water jet machining (AWJM)	Bones	[43–45]
	Zr-based BMG	[46, 47]
	Ti-based alloys	[48–51]
	Stainless steels	[50]
	NiTi alloys	[52–54]
Ultrasonic machining (USM)	Ti-based alloys	[55, 56]
	Zirconia ceramics	[57, 58]
	Natural teeth	[57]
Ion beam machining (IBM)	Biocompatible polymers	[59, 60]
	Ti-based alloys	[59, 61–64]
	Co-based alloys	[59, 61]
	Stainless steels	[61]
Laser beam machining (LBM)	Stainless steels	[65, 66]
	Mg-based alloys	[67]
	Ti-based alloys	[68]
	Biocompatible polymers	[69–72]
	NiTi alloys	[73–76]
	Zirconia ceramics	[77]
	Bioactive glasses	[78]
Electro discharge machining (EDM)	Co-based alloys	[79]
	Ti-based alloys	[79–83]
	NiTi alloys	[84]
	Mg-based alloys	[85, 86]
	Zr-based BMG	[87]
	Ceramic composite	[88]
Electron beam machining (EBM)	Biocompatible polymers	[89–91]
	Dental composites	[92]

various advantages such as no detrimental effects on the generated surface due to no chatter and heat involved, inexpensive and environmentally friendly operation, high machining versatility, and high flexibility with a reasonable good amount of material removal rate [95, 96].

Schwieger et al. [43], in their research work compared an abrasive (biocompatible abrasive) water jet cutting to the oscillating saw of cancellous bone. The performances of the processes are assessed based on the accuracy of dimensional tolerance and the biological potency of the mechanical surfaces of biomaterials (bones). A promising cutting performance in terms of cutting gap angle and surface roughness was achieved, provided that the AWJ machining parameters are optimized. As to the controversial use of biocompatible abrasives because of the safety issues, Dunnen et al. [44] investigated the cutting parameters of pure water jet machining on articular bone. The study showed that water jet technology without abrasives was also feasible and found that 60 MPa was the minimum pressure threshold for the majority of articulate bone tissues. Furthermore, they attempted to predict the hole depth and diameter of the bone based on its local structural properties as illustrated in Fig. 13 [45]. Using regression analysis, the depth and diameter of the holes are correlated to the water jet nozzle diameter and the bone volume fraction as shown in Eqs. 1 and 2, respectively. For a cortical bone, it is recommended to use a nozzle diameter of 0.5 mm to ensure full penetration, whereas a nozzle diameter of 0.2 mm suffices for an articular bone [45].

$$L_{hole} = 34.3\left(D_{waterjet}\right)^2 - 17.6\left(\frac{BV}{TV}\right) + 10.7 \quad \left(R^2 = 0.90,\ p < 0.001\right) \tag{1}$$

$$D_{hole} = 3.1 D_{waterjet} - 0.45\left(\frac{BV}{TV}\right) + 0.54 \left(R^2 = 0.58,\ p = 0.02\right) \tag{2}$$

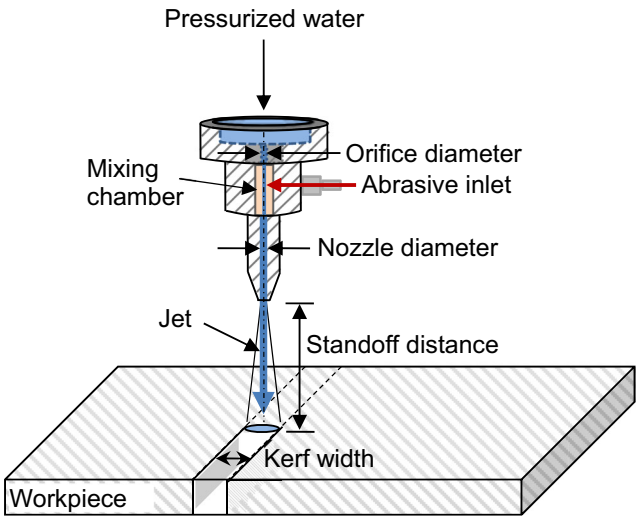

Fig. 12 Illustration of AWJM process

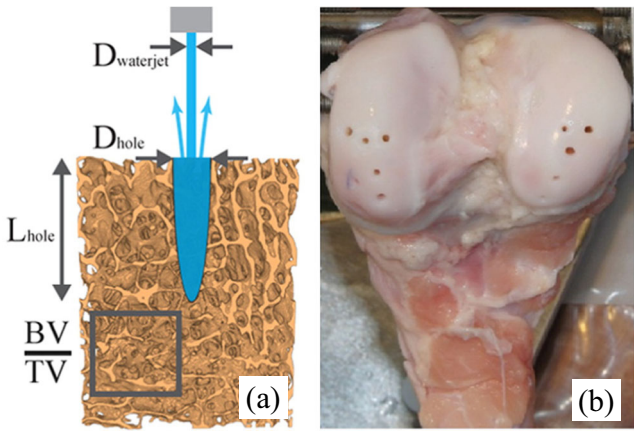

Fig. 13 **a** Illustration of water jet drilling of a bone and **b** water jet drilled holes of pig femur [45]

where L_{hole} is depth of the drill hole, $D_{waterjet}$ is water jet nozzle diameter, BV/TV is bone volume fraction, and D_{hole} is the diameter of the drill bone.

Abrasive water jet machining gives better results in machining Zr-based BMG compared to wire electrical discharge machining (EDM), milling and ns-pulsed laser cutting in terms of surface quality, and transformation of the amorphous phase. The advantages of abrasive water jet (AWJ) process are mainly due to their low process temperatures and higher feed rates. Wessels et al. [46] have compared four different machining processes used in Zr-based BMG ($Zr_{52.5}Cu_{17.9}Ni_{14.6}Al_{10}Ti_5$). From the scanning electron microscope (SEM) images as shown in Fig. 14, it was seen that AWJ produced better surface quality compared to ns-pulsed laser micromachining. The XRD and DSC analysis show absence of crystallization in the surface of AWJ result and chips from dry milling at cutting speed of 20 m/min. In contrast, partial crystallization was seen in the result using wire EDM and chips from dry milling at cutting speed of 200 m/min. In addition, the AWJ process and the lower speed milling process (20 m/min) show no thermal damage compared to milling process at 200 m/min cutting speed.

Another commonly used biomaterials for medical/dental implants and surgical instruments are shape memory alloys (SMAs). Among various based SMAs, the NiTi alloy or Nitinol has been widely used in medical industries especially due to its good biocompatibility [97]. Since it is considered as a difficult-to-cut material, machining of NiTi shape memory alloys brings a real challenging task. Kong et al. [52] attempted to control the depth of penetration during water jet machining of NiTi alloys. They found that the water jet machining process using abrasive particles can have a better depth control than without abrasive particles. This is possibly due to easily strain hardened of martensitic phase at low yield strength for water jet machining without abrasive particles that leads to a non-controllable penetration. In case of water jet machining with abrasives, there were evidence of melts and sparks, thus results in phase transformation from martensite to austenite due to local impacts from high-velocity abrasive particles as illustrated in Fig. 15 [52]. In a forward transformation, the austenite crystal structure changes to twinned martensite at temperature of M_s upon cooling down in a stress-free environment, and completes all the transformation to fully twinned martensite (i.e., 100% martensite) at temperature of M_f. During heating, at temperature of A_s, the twinned martensite transforms back to austenite and results in 100% austenite after temperature of A_f [52]. In addition, with proper control of machining parameters, the abrasive water jet machining can generate surfaces of acceptable qualities to make NiTi shape memory alloys to be used in medical industries [53]. Similar finding was reported by Frotscher et al. [54] during machining of small structures into binary NiTi sheets using water jet machining and micro-milling processes. They concluded that both processes can be used to machine delicate structures, even in very thin NiTi sheets. However, optimizations of cut quality and machining speed are needed to be addressed in order to make the methods more competitive.

Similar to AWJ, abrasive jet polishing (AJP) can be used to improve the surface finish of the biocompatible implants by using combination of abrasive materials, water, and machining oil. Shiou et al. [47] attempted to improve the surface finish of the (Zr48Cu36Al8Ag8) 99.25Si0.75 BMG materials using sequential abrasive jet polishing and annealing processes. In their study, Taguchi's L18 was used to obtain the optimum polishing parameters and the results analyzed using analysis of variance (ANOVA) and the F ratio test. Subsequently, additional improvement of the polished surface finish is achieved using an annealing process in the supercooled liquid region. The surface roughness was measured using atomic force microscope (AFM) within an area of 50 × 50 μm. It was observed that the polishing time, the abrasive material, and the standoff distance have significant effects on the surface roughness in the AJP process while the annealing time and the annealing temperature have important effects on the surface roughness in the annealing process. The surface roughness was improved from an initial value of R_a = 0.675 μm to a final value of R_a = 0.016 μm using the optimal AJP parameters which are SiC abrasive material, 1:5 ratio of abrasive to water, 30° impact angle, 15 mm standoff distance, 2 kg/cm^2 pressure, and 60 min polishing time.

Another method to improve the surface quality of biocompatible materials is to use water jet surface treatment in which high-frequent impact of water drops on the surface causing local plastic deformation, thus producing high compressive

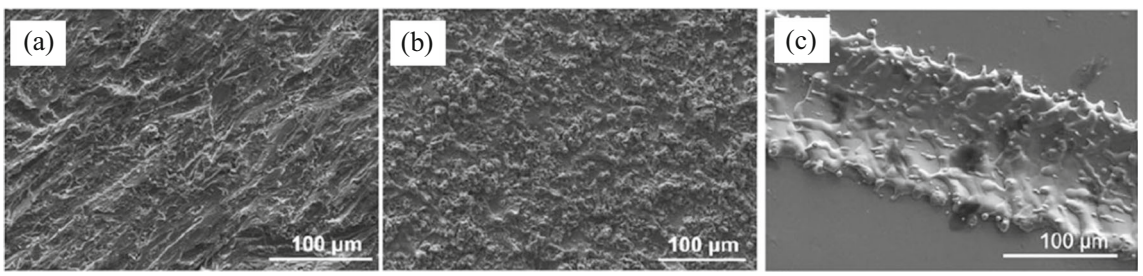

Fig. 14 Scanning electron microscope images of the machined BMG surface using **a** abrasive water jet (1000 mm/min feed rate), **b** electrical discharge machining (EDM) at 380 A, and **c** ns-pulsed laser (1000 mm/s feed rate) [46]

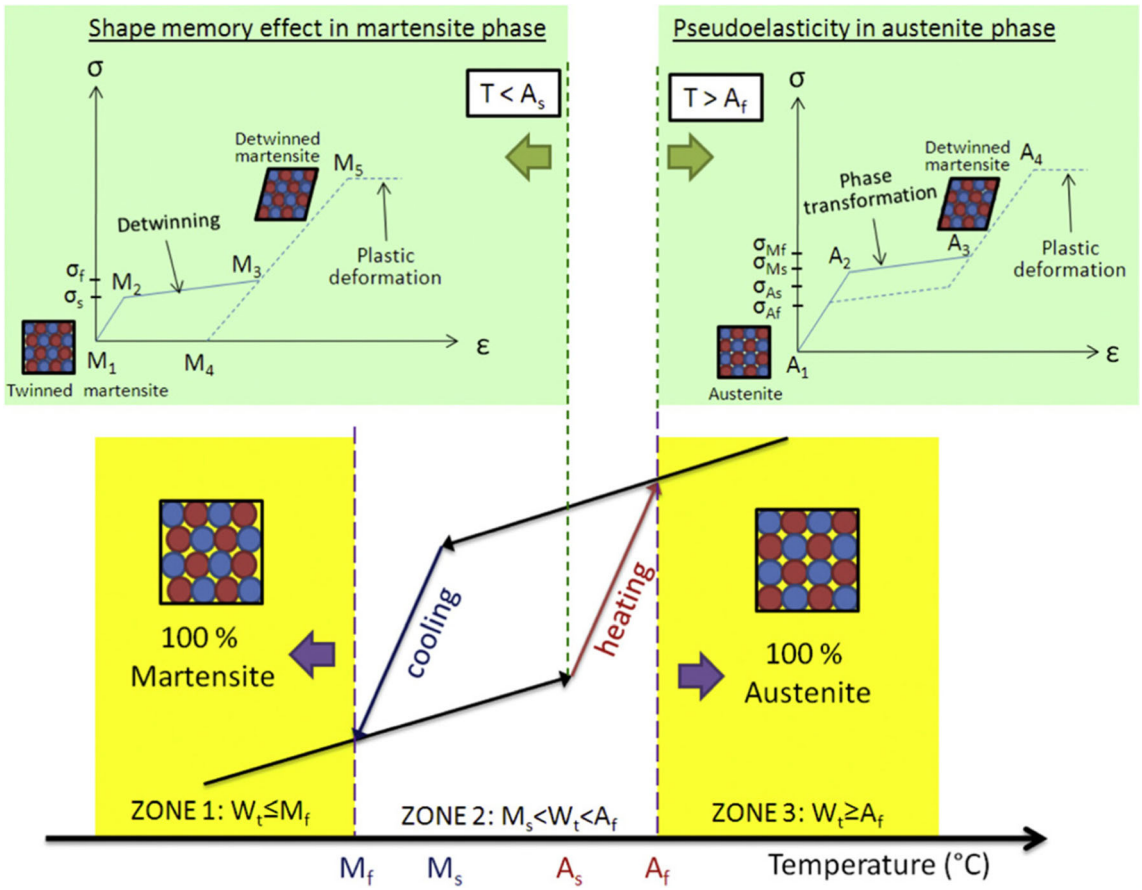

Fig. 15 Phase diagram and stress–strain curve for shape memory effect in martensite phase and pseudoelasticity in austenite phase of NiTi with consideration of water jet operating temperature [52]

residual stresses that leads to enhanced surface hardness and fatigue life [98]. Quite a number of researches in water jet surface treatment have been conducted to study its potential applications and associated sciences. Chillman et al. [48] explored the effects of high pressure water jet at 600 MPa on the surface finish and integrity of biocompatible titanium alloy (Ti-6Al-4V). They varied the traverse rates and the standoff distance. They found that WJP at 600 MPa induces a plastic deformation to higher depths in the subsurface layer and also a higher degree of plastic deformation. Arola and McCain [49] utilized an abrasive water jet to simultaneously texture and work harden the surface of the similar alloy. They found that the surface roughness and the effective stress concentration resulting from AWJ surface treatment of the Ti6Al4V were lower than that resulting from the titanium plasma-spray coating used for cementless arthroplasty. These improvements may facilitate interdigitation of cement or bone and increasing the fatigue life of AWJ-treated biocompatible materials. AWJ surface treatment also resulted in an increase in the fatigue strength of the same alloy [99].

Another study on roughening of AISI 316 LVM and Ti6Al4V by abrasiveless water jet peening treatment was reported by Bariuso et al. [50]. They treated the samples at relatively high water pressure of 360 MPa and moderately slow traverse rates between 50 and 100 mm/min. The higher amount of pits with undercuts and intrusions was observed on the surface of steel specimens especially treated with the lower traverse rate. Furthermore, a significant grain size refinement in the subsurface zone of 10–20 μm depth with about 50% increase of hardness was observed in 316 LVM samples as shown in Fig. 16a. However, the microstructures of Ti6Al4V specimens show slightly different where grain sizes are much smaller with typical biphasic structures consisting of bright zones of V-rich elongated β-phase into a dark matrix of equiaxial α-phase grains as shown in Fig. 16b. Contrary to 316 LVM samples, no change of microstructure between the subsurface layer and the bulk was observed in Ti6Al4V specimens which may explain the absence of subsurface hardening effect. In terms of fatigue strength, a higher value was reported during abrasiveless water jet surface treatment of biomedical Ti6Al4V ELI alloy at a higher water pressure [51]. However, this value is still considered low in comparison of commercial sand blasting-treated sample within the same range of surface roughness [51, 100]. It is believed that the water jet surface treatment may offer an improvement of fatigue strength with a proper optimization of water jet parameters, thus reducing surface defects.

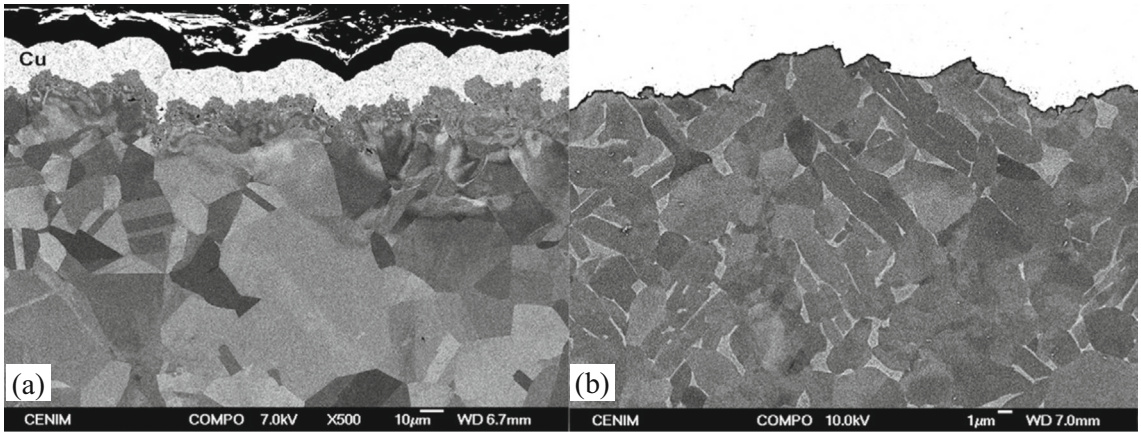

Fig. 16 Backscattered electron images of abrasiveless water jet peened specimens, **a** 316 LVM and **b** Ti6Al4V [50]

3.2 Ultrasonic machining

Ultrasonic machining (USM) is one of the mechanical material removal methods where it has been applied to hard-to-machine and advanced materials. The basic principle of this process is that the material removal process takes place at considerable rate when abrasive particles are ultrasonically vibrated. Due to its superior relative performances, evolving less heat, and cost effectiveness, USM is an attractive technique in the machining of biomaterials [55, 101]. The material removal mechanisms of USM especially on biomaterials have been the subject of various researchers in order to understand the machining behavior. The material removal mechanisms are the combinations of mechanical abrasion by direct hammering of the abrasive particles against the workpiece surface, micro-chipping by impact of the free moving abrasive particles, cavitation effects from the abrasive slurry, and chemical action associated with the fluid employed. Among methods of USM, rotary ultrasonic machining (RUM) is an efficient technique particularly in producing complex contours for hard–brittle materials such as ceramic-based biomaterials. The process combines the material removal mechanism of diamond grinding and ultrasonic machining as illustrated in Fig. 17 [102].

Xiao et al. [57] developed cutting force model in feed direction of rotary ultrasonic milling (RUM) for dental ceramics as shown in Eq. 3.

$$F_f = \frac{K_1^{\frac{3}{4}} \cdot K_2 \cdot C_1^{\frac{1}{4}} \cdot C_a^{\frac{1}{6}}}{C_2^{\frac{7}{4}}} \cdot \frac{\left(a_p - h_e\right) \cdot D_o^{\frac{1}{4}} \cdot v_f^{\frac{3}{4}}}{b^{\frac{1}{4}} \cdot n^{\frac{3}{4}}} \cdot \frac{\left(\tan\frac{\alpha}{2}\right)^{\frac{2}{3}} \cdot H_V^{\frac{5}{3}} \cdot K_{1C}^{\frac{1}{2}} \cdot (1-\nu^2)^{\frac{1}{4}}}{E^{\frac{3}{4}}} \tag{3}$$

where K_1, K_2, C_1, and C_2 are dimensionless constants, C_a is the abrasive concentration, a_p is the cutting depth, h_e is the exposed height of end face abrasive particles, D_o is the outer diameter of diamond metal-bonded core tool, v_f is the feed rate of the core tool, b is the abrasive size, n is the spindle speed of RUM, rpm, α is the angle between two opposite edges of an abrasive particle, H_V is the hardness of workpiece material, K_{1C} is the fracture toughness of the workpiece material, ν is the Poisson's ratio of the workpiece material, and E is the Young's modulus of the workpiece material.

The effective cutting time, material removal volume, and number of active particles in abrasive process were determined during the model development under the assumption of brittle fracture material removal mechanism. According to the model, the cutting force will decrease with the increase in the spindle speed and abrasive size and on contrary with the increase in the feed rate and abrasive concentration which were found consistent with the trends obtained from experiments [57]. Their developed model can be used to predict the cutting force for efficient machining of dental zirconia ceramics during RUM.

Zheng et al. [58] performed an experimental set up to observe performance of ultrasonic-assisted grinding (UAG) in the machining of natural teeth. It was observed that the friction coefficient was reduced and the longitudinal wear depth of

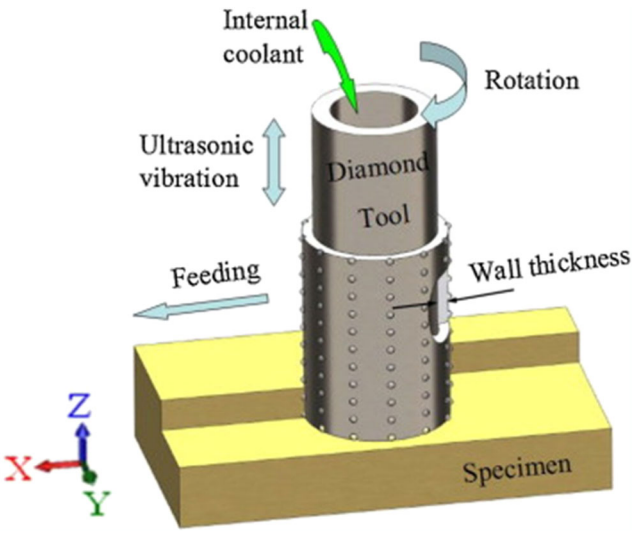

Fig. 17 Schematic view of the USM process [102]

natural teeth decreased when compared to conventional diamond grinding. On the other hand, Chai et al. [56] looked into the effect of ultrasonic vibration grinding which can vibrate longitudinally with a frequency of 20 kHz on the machining performance of USM when compared to conventional grinding method on three selected biomaterials, titanium (Ti-6Al-4V), FCD700, and S45C. Regardless of the material type, it was found that grinding forces decreased as the ultrasonic vibration power and the rotation speed of spindle increased while grinding force was reduced as the feed rate increased.

3.3 Ion beam machining

Ion beam machining (IBM) is the material removal process occurred when charged (ions) are bombarded from an ion source of inert gas towards a specific material to be machined using an accelerating voltage on vacuum chamber. As can be seen in Fig. 18, initially, the ions are generated from a plasma source and extraction grids removed the ion from the plasma and accelerated to the workpiece (biomaterial). Even though the direction of ion beam and mass of the ion are very important factors during IBM, however, effective material removal is achieved when more than 5–10 eV binding energy than the biomaterial atoms are bombarded [103]. The material removal rate (number of atoms removed) is dependent on the type of atoms treated and their energy, angle of incident, and gas pressure used during the process. An approximate size between 0.1 and 10 atoms are removed from the workpiece when an atom (ion) strikes on it. Since the material removal rate in IBM is very low within the range of atomic levels, the process is mainly applied for surface modifications. Two main applications are ion beam figuring (i.e., very fine surface correction and figuring up to hundreds of nanometers) and ion beam smoothing (i.e., polishing to produce ultra-smooth surfaces) [104].

Most research works involving the use of ion beam technology for biomaterials are related to surface modifications. Sioshansi and Tobin [59] have reviewed the application of ion beam-assisted deposition process for surface treatment of biomaterials. They commented that many medical devices are made harder, more wear, and fretting resistant by ion implanting their articulating surfaces. It has been reported further [61] that the surface wear resistance of titanium alloy, stainless steel 316L, and Co–Cr orthopedic prosthesis biomaterials have been improved by hardening the surfaces and hence increasing the coefficient of friction using ion implantations process. Another study has shown that ion beam process on a new kind of Ti-TiC-C gradient biomaterial resulted in remarkable relaxation in the intrinsic stress and thermal stress, thus greatly increased its adhesive strength [62]. While, He [60] investigated micro/nanomachining of biocompatible polymers (*poly*(*methyl methacrylate*)—PMMA) using ion beam lithography. Their results have shown that masked ion beam lithography can change not only the surface topography but also the surface hydrophobicity. This method offers a promising prospect for the fabrication of 2D and 3D microstructures on biocompatible polymers.

Recently, a new method of ion beam-assisted deposition (IBAD) was introduced to improve the adhesion strength between metal and coating for better application in the fields of orthopedics and dental applications. IBAD is a deposition process that adds a thin film layer on the surface of the substrate to form a coating [105]. The process combines evaporation with simultaneous ion beam bombardment to produce adherent dense coatings with virtually any substrate/coating materials combination [105]. Figure 19 shows the schematic diagram of IBAD system [64].

Choi et al. [63] investigated the use of IBAD process for hydroxyapatite coating layer on Ti-based metal substrate. Ar ion beam was focused to the metal substrate to assist deposition of an electron beam vaporizing a pure hydroxyapatite

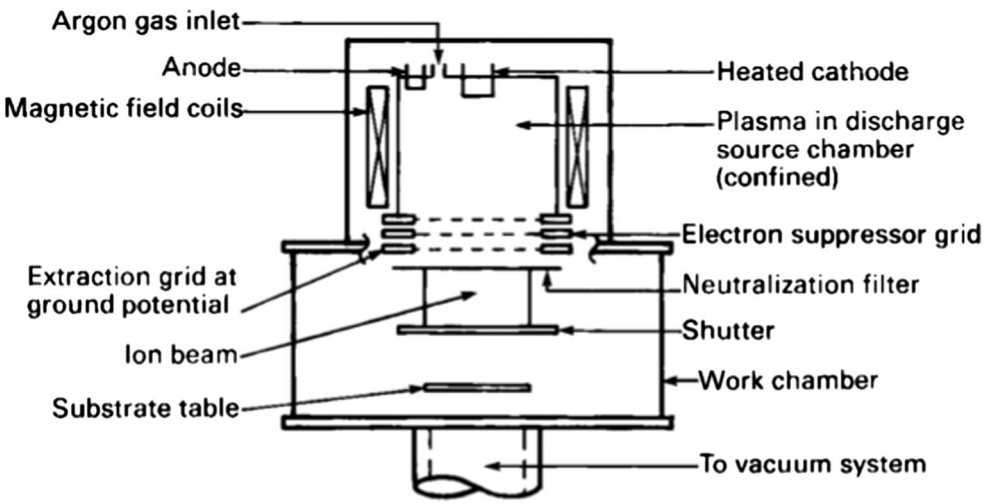

Fig. 18 Components of ion beam machining [103]

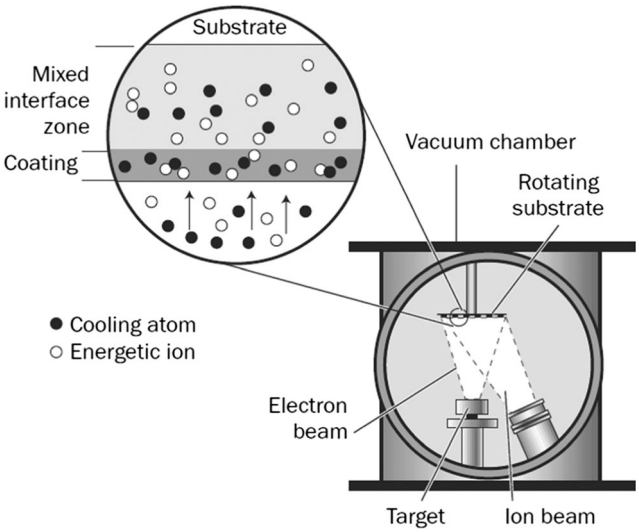

Fig. 19 The schematic diagram of IBAD system [64]

(HA) target. They found that the bond strength between the layer and the substrate increased steadily with an increasing current, while the dissolution rate in a physiological saline solution decreased remarkably. Furthermore, IBAD process of pure titanium screw-type dental implant coated with HA showed more favorable results than a blasted surface as demonstrated by the early formation of osseointegration [64]. The implants were placed in tibia of rabbit and resulted in more rapid osseointegration as well as increased interfacial strength via early skeletal attachment as shown in Fig. 20 [64].

3.4 Laser beam machining

Laser beam machining (LBM) is based on interaction of an intense coherent monochromatic laser beam with a workpiece from which material is removed by melting, vaporization, and chemical degradation [106]. The illustration of laser beam machining process is shown in Fig. 21. The main advantage

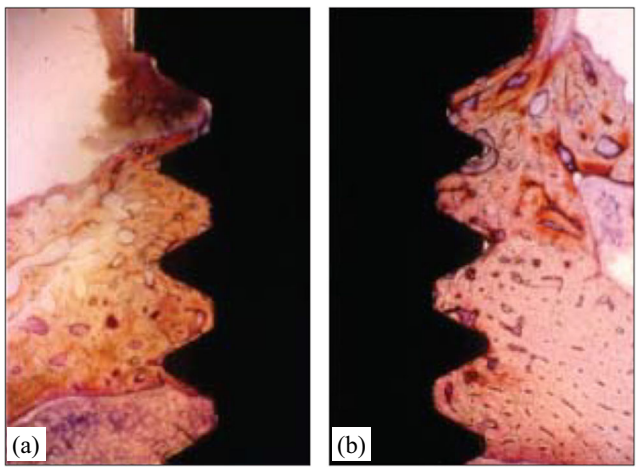

Fig. 20 Histologic views of titanium implants, **a** grit-blasted only specimens and **b** grit-blasted and HA-coated specimens [64]

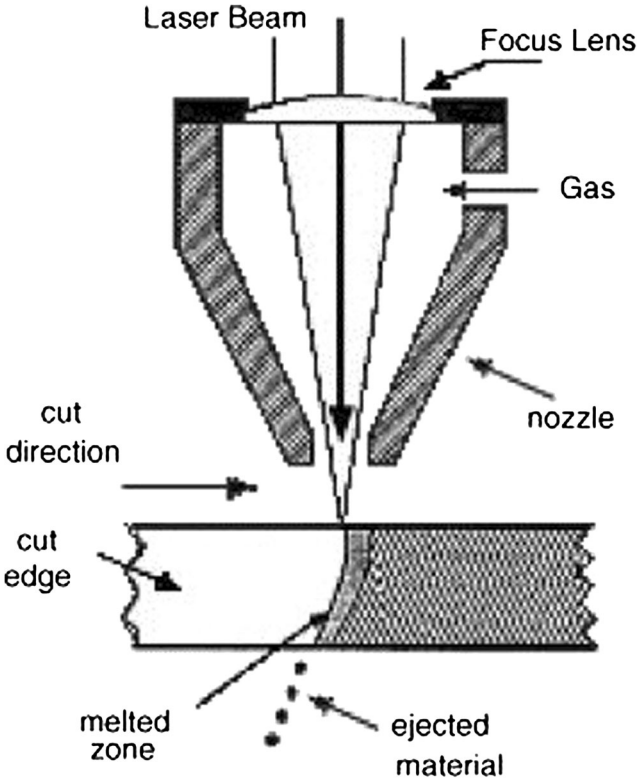

Fig. 21 A schematic of the laser beam interaction with the material [68]

of laser machining is that there is no contact between the tool and the workpiece, thus eliminating the need for secondary operations as usually caused by thrust force and vibration of tools in conventional machining processes. As a result, the process has been widely used in industry to machine almost all ranges of engineering materials including biocompatible metals and non-metals. Based on literature reviews, various types of lasers have been used in materials processing such as neodymium-doped yttrium aluminum garnet (Nd:YAG) lasers, carbon dioxide (CO_2) lasers, fiber lasers, excimer lasers, and ultra-short pulse lasers [107].

Ghany and Newishy [65] investigated the effect of various processing parameters during machining of biocompatible austenitic stainless steel using pulsed and continuous wave Nd:YAG laser beam. They found that the laser cutting quality in terms of kerf width and surface roughness depends mainly on the laser power, pulse frequency, cutting speed, and focus position. Similar finding was reported in laser machining of biodegradable Mg–Ca alloy where a lower laser power resulted in a lower surface roughness and a smaller taper angle due to less thermal damage [67]. Almeida et al. [68] performed experimental work to study the effects of laser processing on the quality in the cut surface of biocompatible titanium alloys. They made a conclusion that although titanium alloys are well known for being difficult to machine materials but selecting the proper laser processing parameters may satisfy all manufacturing needs including edge quality and surface

finish. In order to improve the cutting quality of AISI 316L stainless steel tubes in coronary stents production, Erika et al. [66] used compressed air by passing it through the tube during laser machining process. The amount of dross adhered in the back wall of the tube was reduced because the compressed air was used to drag molten material. Furthermore, fiber laser cutting was successfully used to manufacture stents made from alternative material of biodegradable *polycaprolactone* [69]. The process was able to achieve dimensional precisions with a taper angle lower than 0.033° and a lesser influence upon the material properties owing to the lower absorption of *polycaprolactone* at a 1.08 μm wavelength fiber laser. A higher energy density input, E_{laser} produced by the beam resulted in a lower accuracy of cut due to the heat accumulated in the nozzle produces the melting of adjacent zones generating unpredicted results in some zones as demonstrated in Fig. 22 [69].

In case of machining of Nitinol alloy, Fu et al. [73] applied an improved process using fiber laser cutting instead of conventional laser cutting. Results indicated that the fiber laser cutting produced much less thermal damage on surface integrity due to the high beam quality. In terms of machining parameters, it was found that laser cutting speed showed a much higher influence on surface integrity than laser power intensity. A higher cutting speed caused insufficient rejection of molten material, thus produced high surface roughness and a thick recast layer [73]. Hung et al. [74] proposed a NiTi tube curve surface process involving a femtosecond laser process and a Galvano-mirror scanner as illustrated in Fig. 23. They found that the curve machining efficiency was doubled by altering the laser movement path to a wider kerf line enabling the assisted air to remove the debris deposited at the bottom of the kerf. They concluded that altering the machining path using the scanning system can decrease the production of heat-affected zones in medical device applications. They further utilized a unique characteristic of Gaussian beam of femtosecond laser with aligning the edges which consequently producing rounded-shaped edges from squared edges with precise dimension [75].

More recently, laser surface treatment has been applied as a method to modify the surface properties of biomaterials. Laser surface texturing was applied to improve surface characteristics in terms of wettability, roughness, and morphology of biomaterials especially in the case of polymers such as *polyether-ether-ketone* (PEEK) [70], *ultra-high-molecular-weight polyethylene* (UHMWPE) [71], and *polypropylene* (PP) [72]. Results suggest that laser texturing with nanosecond wavelengths is suitable to increase the surface roughness higher than 1 μm [72, 108]. This is the minimum required value to improve the bone bonding to the implant surface [108]. Furthermore, it was found that the laser treatment does not substantially modify the mechanical properties of textured surface [72]. Moura et al. [77] reported that the laser surface texturing of zirconia-based implants demonstrated better wettability, better aging performance, and better primary stability as compared to the traditional surface treatments using sand blasting and chemical etching. Laser surface texturing has also been applied to modify surfaces of 45S5 bioactive glasses using a nanosecond Nd:YAG laser at different laser fluence levels [78]. Experiments indicated that the glass samples

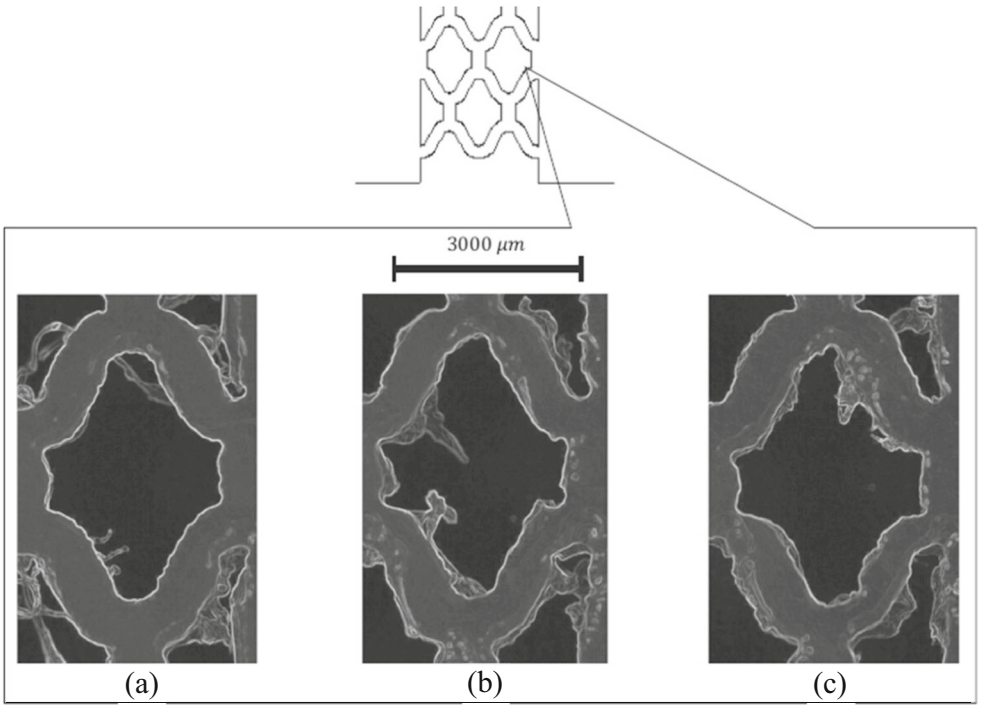

Fig. 22 Precision according to E_{laser}, **a** 1.00E + 09 J/m^2, **b** 1.85E + 09 J/m^2, and **c** 2.91E + 09 J/m^2 [69]

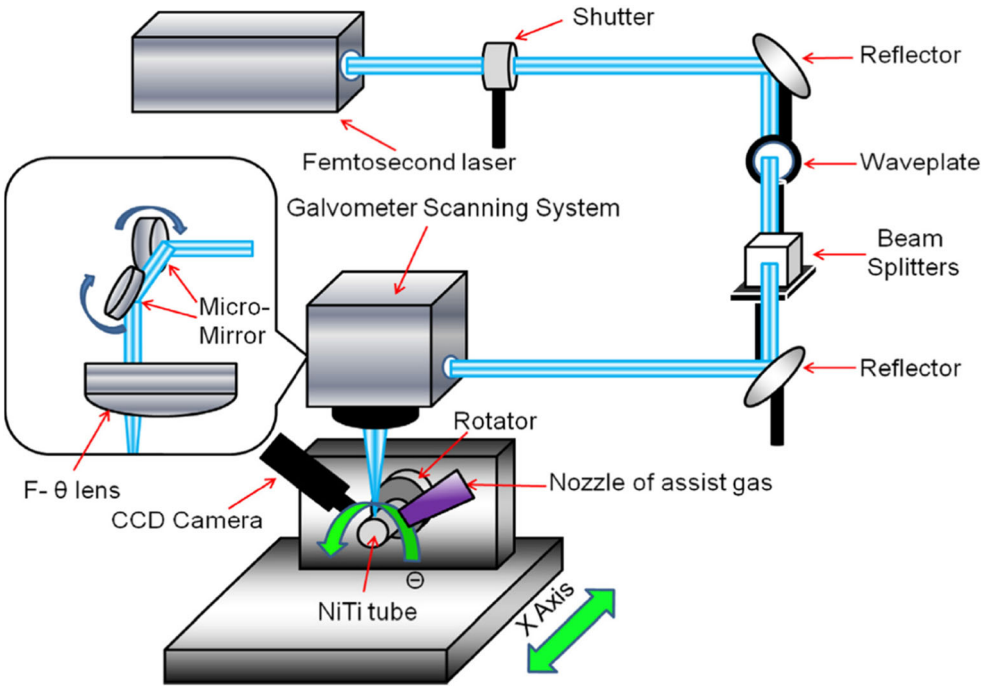

Fig. 23 A schematic illustration of femtosecond laser ablation system on NiTi tube [74]

experienced the formation of porous microstructure with pore size varying from 50 nm to 2 μm, thus increasing in surface area, thereby facilitating the interactions with body fluid. Laser surface treatment has also shown that it is able to enhance the wear resistance of NiTi alloy surface used for orthopedic applications using laser diffusion gas nitriding [76]. It can be concluded that laser surface treatment is an attractive and effective means for modifying surfaces of implant materials in biomedical industries.

3.5 Electrical discharge machining

Electrical discharge machining (EDM) applied in the processing of dentals or implants is a thermoelectric process where the implant is immersed in a liquid (dielectric fluid) made up of the cathode of the electrochemical cell, with Cu implant analogues serving as an anode. Ntasi et al. [79] demonstrated that the biomedical materials such as Co–Cr (Okta-C) and a grade II cpTi (Biotan) alloys subjected to EDM process showed a decrease in corrosion resistant in both materials that may result in severe biological reactions. This has been experimentally observed that the morphology of the implant has been changed and the contents of Mo, Cr, Co, Cu (Co–Cr), and Ti, Cu (cpTi) had decreased while the carbon content increased. This unwanted precipitation of external materials on the biomaterials has been illustrated more by the works of Theisen et al. [84]. They have demonstrated that EDM has a more significant effect on the surface texture of the pseudoelastic NiTi shape memory alloys (SMAs). This has been done using a copper–tungsten (CuW) electrode so that the surface structural integrity was modified. The tungsten carbide was observed at the surface of the biomaterial that enables the NiTi materials to be stable in different applications. However, additional surface finishing using machining with low process energy or by electrochemical removal of the melting zone has to be applied in order to remove some unwanted materials and structures on the heat-affected zone of the EDM process. The use of EDM machining process on orthopedics implants of Ti-6Al-4V alloy was also reported by Strasky et al. [82]. The high carbon deposition, lower strength, and poor fatigue were observed. The EDM process has produced better substrate for the adhesion and growth of human bone-derived cells than the alloy plasma-sprayed with TiO_2. This also shows a post treatment such as heat treatment and finishing process to remove unwanted materials from the surface of the biomaterials need to be conducted in order to fully use the EDM process. Otsuka et al. [83] compared the osteoblast response on the biocompatible titanium surfaces produced using EDM and traditional machining processes as shown in Fig. 24. They found that EDM machined surface produced better osteoblast cell responses in promoting cell attachment and differentiation on the Ti surfaces due to its high super hydrophilicity but did not affect cell proliferation.

Various technologies or methods have been induced in the EDM machining processes in order to reduce the heat-affected zone of the biocompatible implants, prevent the unwanted decomposition of harmful elements, and improve the surface roughness. Klocke et al. [86] reported that EDM machining process is well suited for the creation of geometries with high aspect ratios and microstructures for biomaterials as seen in Fig. 25. Furthermore, they reported that in the wire EDM machining of magnesium alloys for biodegradable orthopedic

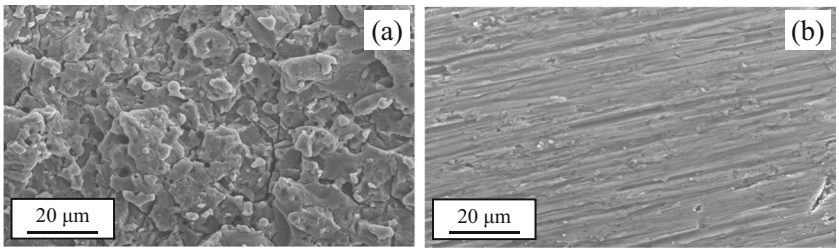

Fig. 24 **a** SEM image of EDM machined surface with complicated and crater shaped structures as well as electrical discharge grooves. **b** SEM image of a machined surface with linear grooves [83]

implants, finishing operation produced a surface with no detectable foreign materials unlike roughing operation where very little foreign materials originating from the used electrode was detected [85]. In case of die sinking EDM, no foreign material was detected besides the base material which later confirmed with the results of in vitro toxicity test.

In other experimental research works by Gu et al. [81], a new type of bundled die sinking electrode was designed to improve the EDM machinability of Ti-6Al-4V biocompatible material to be used in different medical implants. The bundled electrode was achieved by discretizing the solid die sinking conventional electrode into a 3D tubular structure shown in Fig. 26. With this setup, the machinability of the material has significantly improved in terms of the material removal rate (MRR), the discharge rate, and the tool wear rate (TWR). More importantly, the amount of carbon and some unwanted material deposition on the work piece and electrode surfaces were radically reduced than the conventional solid electrode based on the energy dispersive x-ray spectroscopy (EDS) results. This reduced deposition of carbon was achieved due to the better flushing of the die electric material used during the EDM machining. The minimal deposition can be eliminated using further finishing operations such as wire EDM and plasma electrolytic conversion of the surface [85].

Due to the temperature sensitivity of the BMG materials which can cause crystallization, the heat generated by the machining process needs to be considered. The change of their amorphous phase can degrade the mechanical and chemical properties. Therefore, micro-EDM having low discharge voltages and capacitances is more suitable to be used compared to conventional EDM. The high discharge energy produced by conventional EDM will generate high heat, which in the end produce crystallization. The application of the micro-EDM on $Zr_{41.2}Ti_{13.8}Cu_{12.5}Ni_{10}Be_{22.5}$ BMG materials have been conducted by Huang and Yan [87]. It is observed that the micro-EDM process on Zr-based BMG at low discharge voltages (70 V) and capacitances (220 pF) produced smaller craters and recast layers, reduced the surface roughness; however, it lowed the material removal rate. They argued that the process only produced very small crystallization on the surface due to the low discharge energy.

Bucciotti et al. [88] reported the suitability of producing biomedical implantable components from electro-conductive silicon nitride/titanium nitride (Si_3N_4-TiN) composite using EDM process as shown in Fig. 27. They concluded that the composites produced by hot pressing are suitable to be used in load-bearing prosthesis due to its favorable microstructural and mechanical properties. Furthermore, these composites can be successfully manufactured very complex near net-shapes even with undercuts using EDM process.

3.6 Electron beam machining

Electron beam machining (EBM) is defined as a thermal machining process where high-velocity electrons discharged from a narrow beam, thus instantly heat, melt, or vaporize the surface of materials [109]. The applications of EBM have expanded over the years due to the different range of energies available which include machining, welding, lithography, additive manufacturing (melting), and finishing [110]. In this subchapter, the emphasis is given to report results involving machining operation especially drilling and lithography. Other applications of EBM such as additive manufacturing are discussed later in "Additive manufacturing" subchapter. The schematic illustration of EBM process is shown in Fig. 28. Initially, high-velocity electron particles are generated

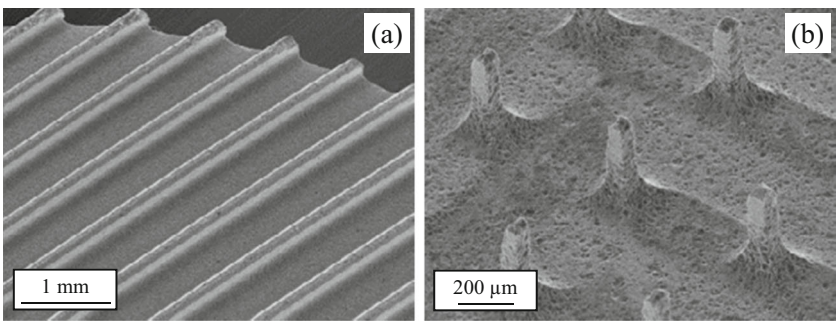

Fig. 25 **a**, **b** Two examples of EDM machined structures of biodegradable magnesium [86]

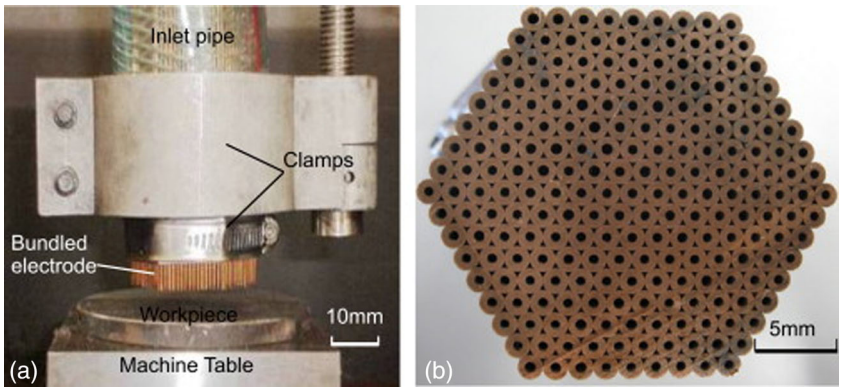

Fig. 26 **a** A 3D tubular structure of electrode setup and **b** end view of electrode [81]

from a cathode filament which later move towards an anode so that they do not diverge from its path. Finally, a high intensity electron beam is directed and focused to impinge on the workpiece by passing them through a series of lenses.

Similar to ion beam technology, most applications of electron beam technology for biomaterials are associated to surface modifications. Park and Lee [89] used a large pulsed electron beam to modify the surface of PMMA samples. Their results have shown that an increase of 40% in the visible light transmission and 30% decrease of surface roughness for irradiated samples were reported. Also, the irradiated PMMA sample had a high surface tension and low water contact angle which make them suitable to be used for dental components. Another study for dental composites, Behr et al. [92] reported a significant increase of fracture toughness, hardness, and wear resistance for different commercial veneering composites after electron beam treatment. However, some color changes were observed which can limit the use of electron beam treatment for dentistry. Faltermeier et al. [90] attempted to improve the mechanical properties of polymeric orthodontic brackets using electron beam irradiation. They found that *polycarbonate* and *polyurethane* samples showed an improvement of fracture toughness and hardness after electron beam treatment. In contrast, *polyoxymethylene* samples could not be improved by electron beaming due to its already high fracture toughness and hardness.

In case of *polyether-ether-ketone* (PEEK) coated with a pure titanium layer using an electron beam deposition method, the biocompatibility and adhesion to bone tissue have been

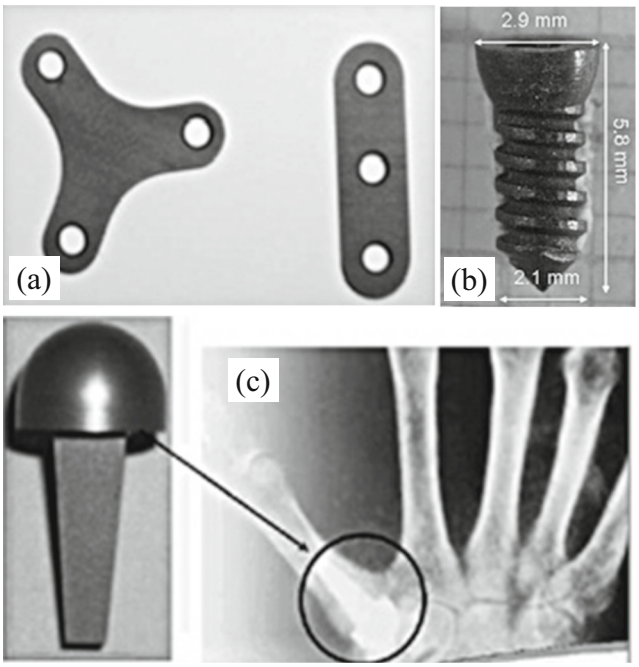

Fig. 27 Example of components produced by EDM process from hot pressed Si_3N_4-TiN billet, **a** plate, **b** screw, and **c** basal thumb implant [88]

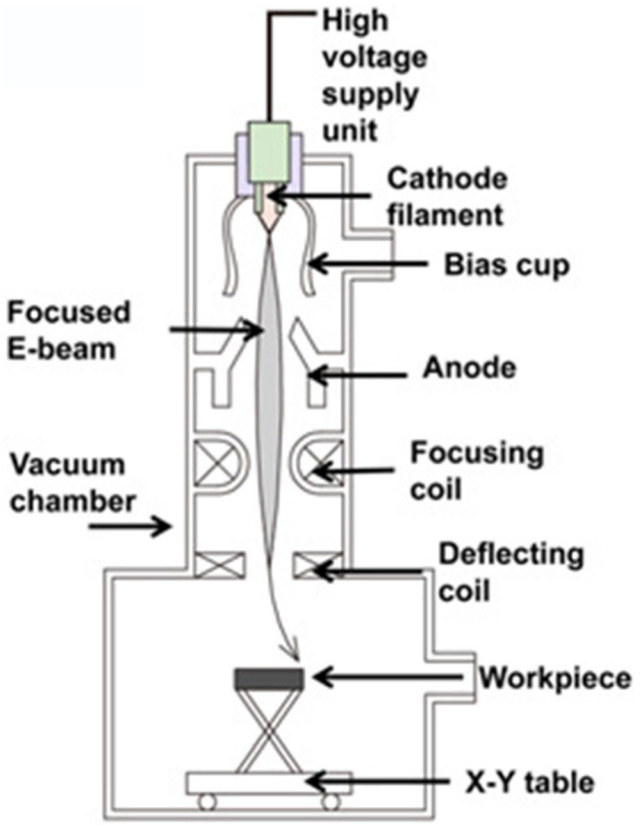

Fig. 28 Schematic of continuous electron beam machining process [110]

remarkably improved [91]. The in vivo animal tests using the rabbit tibial model showed that the Ti coating enhanced the osteoconductivity of PEEK as shown in Fig. 29 [91].

It is interesting to realize that all these non-conventional machining processes have shown a remarkable success in machining of biocompatible materials. They are being used in various applications including in medical industry. However, these processes have their own drawbacks regarding workpiece materials, shapes, sizes, economical aspects, quality of cuts and others. Table 3 shows the comparison of main advantages and disadvantages of various non-conventional machining processes.

4 Current status and future trends of machining of biocompatible materials

The machining of biocompatible materials becomes a challenging task due to the need for smaller size, tighter accuracy, complex shape, and lower surface finish. For example, fixture design for machining setup may be needed due to the structure and shape complexity of biocompatible materials of implants (prosthesis) which is a challenging task by itself. In addition, the surface characteristics of certain shapes in biomaterial implants such as threads and grooves are affected by the quality of machining process. For instance, the surface roughness obtained through machining has an effect on bone-implant interface which affects the mechanical interlocking of bone and enhancement of the shear strength [120]. The machining of biocompatible materials using the conventional and non-conventional processes discussed in "Conventional machining of biocompatible materials" and "Non-conventional machining of biocompatible materials" sections are more challenging and more difficult due to the fact that biomaterials have to be converted into complicated geometries with improved mechanical properties. In addition, the machining process improvement can also be simulated using finite element analysis (FEA) method especially in order to predict the effect of cutting parameters on the machining process. Accordingly,

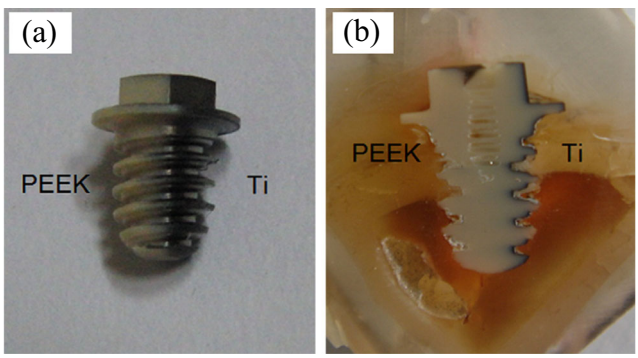

Fig. 29 Optical images of half-coated Ti on PEEK screw, **a** before implantation and **b** after harvesting [91]

the following machining technologies and strategies have been recommended.

4.1 Micro-scale machining

Machining biomaterial surfaces in a micro range, for example, surface modification of micro-bio-interfaces to improve the compatibility of implants and cell tissues, is one of the state of the art process worth to be discussed and investigated. Many fabrication methods have been developed to produce micro-size biomedical components with most of them are reported using micro electro mechanical system (MEMS)-based process such as dry etching, lithography, electroplating, *Lithographie Galvanoformung Abformung* (LiGA). Non-conventional-based micromachining such as laser ablation technology have also been reported [121, 122]. The demands for accurate and precise medical devices and implants especially having micro-scale features can be solved by using micromachining methods. One of the potential methods to produce micro-features of biomaterials is mechanical micromachining (micro-cutting). Fabrication of micro-features and micro-components using micro-cutting such as micro-milling has some advantages over MEMS-based processes such as capability to manufacture 2D, 2.5D, and 3D features with high aspect ratio, flexibility and simplify the production of micro-parts and micro-components, and ability to process a wide range of materials [123]. In addition, micro-cutting can avoid the use of hazardous chemicals, reducing operational and investment costs.

In the micro-milling of titanium alloys such as Ti-6Al-4V, burrs formation, tool wear, and surface quality are the main issues that need to be considered. Burr formation in the micro-scale milling is more obvious since the size of burrs can be comparable with the size of micro-features being produced [125]. Nevertheless, burrs formed in the micro-milling process can be reduced using tapered tools [126]. The use of cBN-coated tungsten carbide (WC/Co) tool in the micro-milling Ti-6Al-4V can reduce the tool wear, lower surface roughness, and produce less burrs [28]. The cBN-coated tungsten carbide tool showed better performance compared to uncoated tool mainly due to the low temperature in the tool caused by lower friction coefficient and higher effective thermal conductivity.

Microstructure has significant effect on the cutting mechanisms and surface quality in the micro-scale machining process [124]. Atanasio et al. [124] studied the effect of Ti-6Al-4V titanium alloys microstructures on the micro-milling process. Four different microstructures (namely bimodal, fully equiaxed, fully lamellar, and mill annealed) were obtained through recrystallization annealing treatments carried out at different times and temperatures as shown in Fig. 30. Micro-channels were produced using tungsten carbide (WC-Co) titanium aluminum nitride [(Ti, Al) N]-coated two flute flat

Table 3 Comparison of main advantages and disadvantages of non-conventional machining processes

Process	Advantages	Reference	Disadvantages	Reference
Abrasive water jet machining (AWJM)	Highly productive and cost-effective for machining of hard and brittle materials	[48, 111]	Challenge to have a better depth control during machining	[52]
	Absence of thermal effects	[49, 99, 112]		
Ultrasonic machining (USM)	Suitable for machining of hard and brittle materials	[55, 57, 101]	Low machining rate	[55, 101]
	Less heat involved	[101]	Not suitable for deep hole machining	[55]
Ion beam machining (IBM)	Easily controlled of deposition rate	[59, 105]	High cost of the equipment	[104]
			Low processing time	[104]
Laser beam machining (LBM)	Used for machining complex profiles for almost whole range of materials	[65, 106, 113]	Thermal effects (e.g., heat affected zone, recast layer) of machined samples	[106, 113–115]
	Suitable for machining of small features	[66, 74, 75]	Low machining time	[106, 107]
Electro discharge machining (EDM)	Suitable for machining of complex shapes with good machined quality	[84–86, 116]	Thermal effects (e.g., heat affected zone, recast layer) of machined samples	[79, 115]
			Suitable for highly conductive materials	[74, 117]
			Low machining rate	[74, 79, 87]
Electron beam machining (EBM)	Suitable for miniature components due to high machined accuracy	[89, 110]	High cost of the equipment and the length of time required for machining	[118]
			Limited size of workpiece due to the size of vacuum chamber	[92, 110, 119]

end mills with a diameter of about 200 μm and a length of cut equal to 300 μm. The cutting speed was 25,000 rpm (15.7 m/min), the depth of cut was 50 μm, two different feed per tooth were used (0.5 and 1.5 μm/tooth), and tests were conducted in dry cutting condition. Design of experiment (DOE) analysis was conducted in order to observe the effect of material microstructure, feed per tooth, and windows position on the cutting force.

It was observed that material structures affect the micro-milling process and the surface quality especially burrs. Less burrs were observed when micro-milling a bimodal structure. The micro-milling of lamellar microstructures produced better process stability in terms of lower scatter, lower cutting forces, and less tool wear. The lowest cutting force was measured when milling the fully lamellar microstructure, while the highest for the fully equiaxed microstructures due to the fact

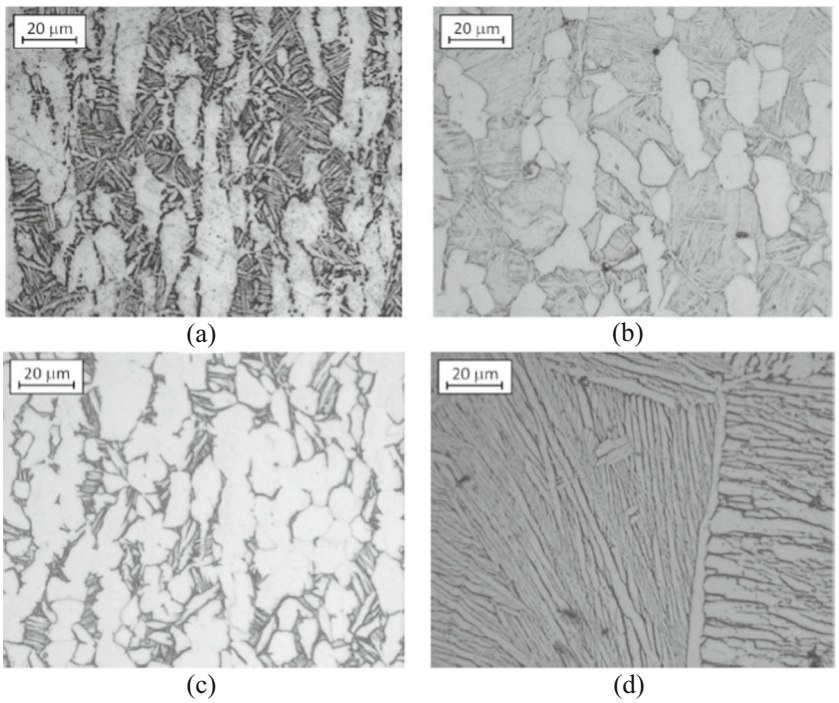

Fig. 30 Optical microscope images of Ti-6Al-4V microstructures used in the micro-milling experiments: **a** mill annealed, **b** bimodal, **c** fully equiaxed, and **d** fully lamellar [124]

that the lamellar structures is softer than the equiaxed structures. The largest scatter of force values was observed in the case of bimodal microstructure. However, at low feed rate (0.5 μm/tooth), tool run-out and plowing affect the cutting forces.

In the micro-milling of shape memory alloys (SMA) NiTi using 0.4-mm solid carbide, the application of minimum quantity lubrication (MQL) combined with high feed rate and high width of cut can improve the surface quality, reduce the burrs, and extend tool life [25]. Micro-scale columns and webs have been successfully produced by applying optimum cutting parameters which are cutting speed 33 m/min, feed per tooth 12 μm, depth of cut 10 μm, width of cut 40 μm, and additional MQL coolant (Fig. 31).

Piquard et al. [26] also have attempted to study the significant parameters that affect the burr formation especially top burrs in micro-milling of NiTi alloys such as seen in Fig. 32. A DOE analysis was conducted on six parameters: strategy (up or down milling), depth of cut, cutting speed, alloy (austenitic or martensitic), feed per tooth, and width of cut. It was observed that height and width of burrs are mainly affected by feed per tooth and width of cut with a low cutting speed, an up milling strategy, and a high feed per tooth produced less burrs.

Frotscher et al. [54] reported the comparison between micro-milling and water jet machining on delicate structures such as very thin NiTi sheets. In this study, the workpiece is binary pseudo-elastic NiTi sheets (380 × 80 mm) with a Ni-content of 50.9 at. % and a thickness of 0.1 mm (oxide free surface). The non-abrasive precision water jet machining with a 37-kW pressure pump, a maximum nominal pump pressure of 400 MPa, a collimator tube type 3DS, and sapphire nozzles with a focusing diameter of 0.08 mm was used. The abrasive cutting was performed using SiO_2 abrasive (mass flow rate of 25 g/min, mesh no. 120 and no. 220) at pressure 50–380 MPa. In the micro-milling experiments, the cutting tools were solid carbide end mill coated with a thin TiAlN layer having a diameter of 0.4 mm in order to generate a minimum strut thickness of 0.2 mm. The cutting speed was varied in the range of 25–37 m/min and the feed was constant at 131 mm/min. The cutting depth was increased from 10 to 100 μm. Experimental results show that non-abrasive water jet machined surface has a wavy nature caused by vibrations of the thin sheet due to the absence of supporting fixture below the sheet as shown in Fig. 33a. It has been reported that the supporting fixture has major roles in the micromachining thin workpieces [127]. While the micro-milled surface has better quality, some burr formation was observed as shown in Fig. 33b. Water jet machining is seen to be better in terms of overall cutting time, thermal influence of the work piece, and operating costs. Whereas, the

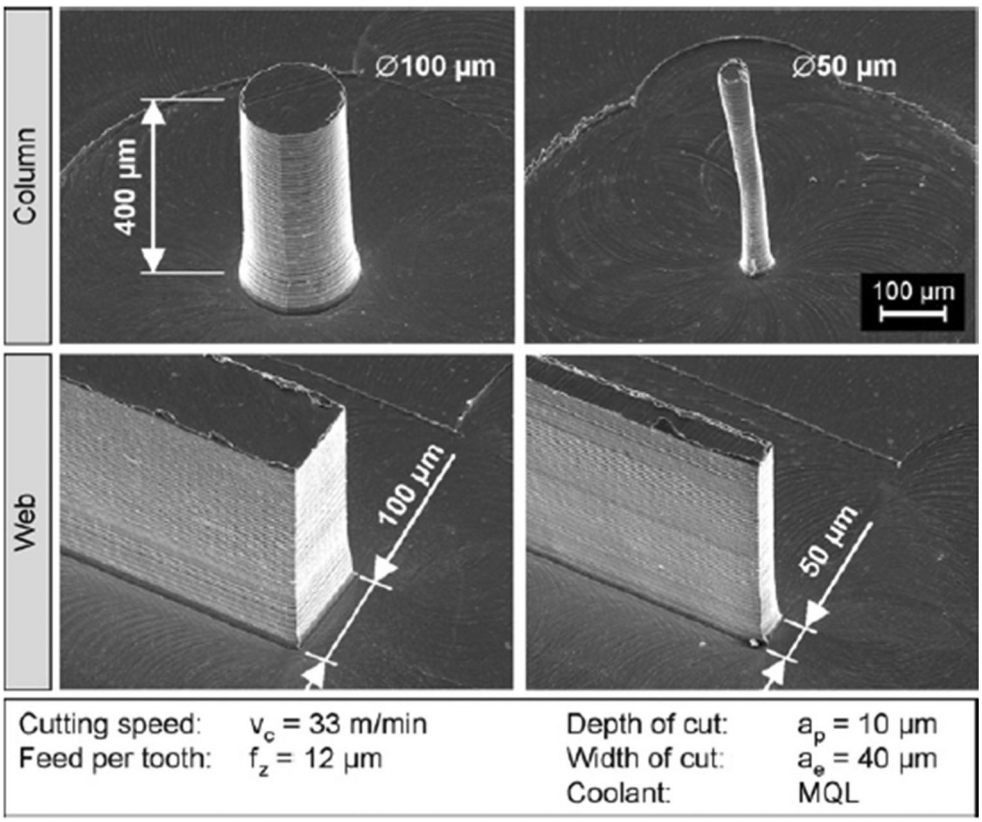

Fig. 31 Columns and webs produced by micro-milling on SMA NiTi workpiece [25]

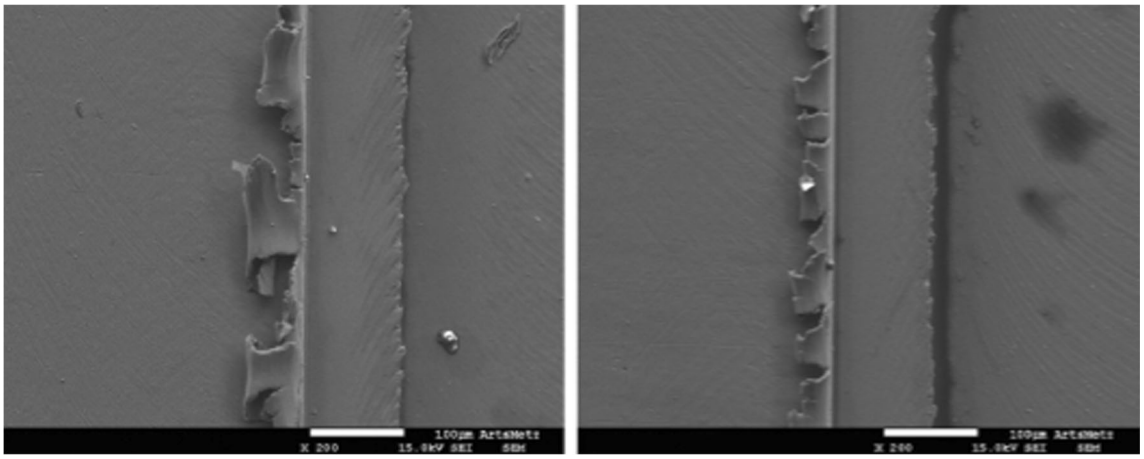

Fig. 32 Top burrs occurred in the micro-milling of NiTi alloys [26]

micro-milling process can achieve better shape accuracy but deburring such as electro-polishing is needed in order to achieve good surface finish for medical applications.

Bakkal and Nakşiler [31] investigated the effect of feed rate on cutting force, burr formation, and surface roughness on meso-milling of Zr-based bulk metallic glass ($Zr_{52.5}Ti_5Cu_{17.9}Ni_{14.6}Al_{10}$. BMG). Slot-end milling experiments were used to observe the mechanics of meso-milling processes of Zr-based BMG and compared with SS304 and Al6061-T6. The tool was 1-mm diameter uncoated solid WC end mills with two cutting edges. The fix depth of cut and spindle speed were used with the values of 0.5 mm and 5000 rpm, respectively. Various feed rates were 0.25, 0.5, 1, and 2 μm per tooth. It is observed that the cutting force in the machining BMG is less than SS304 but more than Al6061 under the same conditions. From the range of the observed feed rate used in their experiments, they found that the lowest feed rate gives the best surface roughness, less burrs, and lower forces.

There are not many literature specifically discussed about the machining of polymers to be used for biocompatible components. Ervine et al. [128] have studied the micro-milling of acrylic polymers which are p*henyl ethyl acrylate* (PEA) and p*henyl ethyl methacrylate* (PEMA) copolymer. The focus of their work is on surface quality especially burr formations encountered during micromachining of these biomedical grade polymers. A tungsten carbide single fluted cutter was used with the following geometry, rake angle: 0°, helix angle: 0° and relief angle: 30°. The cutting edge radius of the tool is approximately 1 μm and a nose radius is 6 μm. Two sets of

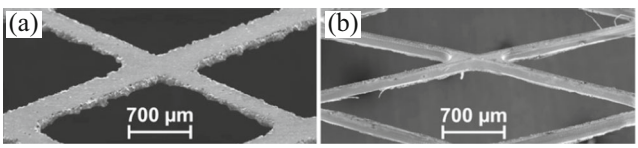

Fig. 33 Upper side of a machined stent-like structure using **a** non-abrasive water jet and **b** micro-milling [54]

experiment were conducted. First set was conducted using constant depth of cut at 0.7 mm and feed rate at 2 mm/s but using various spindle speed starting from 20,000 to 100,000 rpm in steps of 5000 rpm. The second set experiment used constant depth of cut and spindle speed, 0.7 mm and 35,000 rpm, respectively, with the feed rate varied between 0.5 and 8 mm/s (0.86–13.71 μm/rev).

The experimental results show that burr formation and edge overcut occurred at low speed due to the lacks of stiffness as shown in Fig. 34a, b. At higher spindle speed, materials deposition and edge damage are greater especially due to the effect of thermal on the material behavior. Further increases in cutting speed resulted in fully groove clogging due to the embedded polymer debris as shown in Fig. 34d. The low feed rates produced slots with internal surface damage and groove clogging as shown in Fig. 34c, d. At high feed rates, significant burrs occurred on the down-milled surface of the groove. And at higher feed rate, bulk deformations were occurred producing tear burrs and poor machined geometries. At the levels chosen, moderate speeds of 30,000 to 40,000 rpm, and low to moderate feeds between 2.5 and 3.5 mm/s produce the best machining outcomes in terms of surface damage.

Study on the micromachining of biocompatible materials was not only reported on the bulk or raw materials but also on the additive manufacturing products. Rysava et al. [129] have conducted experimental work on the micro-drilling and threading of Ti-6Al-4V dental pin produced by direct metal laser sintering (DMLS). The analyses are mainly on the effect of cutting speed and feed rate to the surface quality of the 1.6-mm diameter tungsten carbide uncoated micro-drilling and the single point threading. The results show cutting speed of 60 m/min and feed rate of 10 μm is the optimum parameter for better hole quality (Fig. 35).

In summary, micro-milling was proved to be a suitable machining process to produce micro-products. This section showed the research works of various micro-mechanical

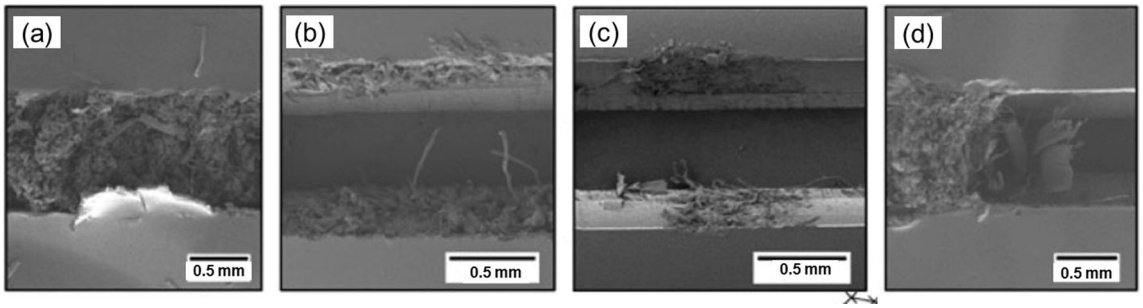

Fig. 34 The surface quality produced in the micro-milling of the biomedical grade polymer, **a** burr formation, **b** edge overcut, **c** internal surface damage, and **d** groove clogging [128]

micromachining in establishing an understanding between the process parameters (spindle speed, feed rate, depth of cut, tool diameter), microstructure of surfaces, and the performance parameters such as accuracy, surface finish (burr), and geometrical qualities. The burr formation (size or volume) has been the issue and its removal process, in that case, the analytical models has to be developed as future research works in order to predict and to take the necessary measures.

4.2 Simulation and modeling of machining biomaterial using finite element analysis

In order to get a thorough understanding and to predict the behavior of biocompatible materials during machining, numerical investigation using simulation, and modeling has become an interesting research topic. Finite element analysis (FEA) was normally used to simulate and model various machining processes of biomaterials. The focus is mainly on the effect of the cutting parameters on the forces [130] and tool wear [131]. The general FEA procedure is shown in Fig. 36. Initially, the geometric modeling of the biomaterial workpiece and machining tool is designed. Subsequently, the material properties of the workpiece and tool and machining parameters are selected. After that, meshing, selecting element size, and applying boundary conditions are conducted. Machining simulations are conducted and output such as forces, temperature distribution, and chip flow are analyzed. Validation of the results is normally conducted in order to ensure the developed model and simulations are the same with the experimental results.

The tool wear in machining Ti-6Al-4V was studied by using finite element analysis. Chiappini et al. [133] built a finite element model of Ti-6Al-4V turning using Deform2D™ in order to simulate sinusoidal spindle speed variation (SSSV) and constant speed machining (CSM) processes. Figure 37 shows the tool and workpiece setup used for the simulation. The model was validated by experimental turning tests in dry orthogonal conditions of Ti-6Al-4V tubes. Initially, a thermo-mechanical simulation was conducted to predict cutting forces and temperature both in the workpiece and at the tool–chip interface. A thermal only simulation was also performed (just for SSSV case) to predict the temperature distribution inside the tool during cutting at the steady state conditions. In the simulation, the Cockroft–Latham fracture criterion with a critical damage value of 245 MPa was adopted. Nominal cutting speed of 40 m/min, spindle speed modulating frequency of 2 Hz, and nominal feed rate equal to 0.3 mm/rev were used. Since the elastic spring back of the workpiece material was not considered in their model, thrust force extracted from the simulations was seen to be underestimated. It was found that the tool–workpiece engagement varies according to the chip thickness modulation in spindle speed variation machining. This affects the heat generation (due to material deformation) and the heat flows both in the tool and the workpiece. At minimum cutting speed (the

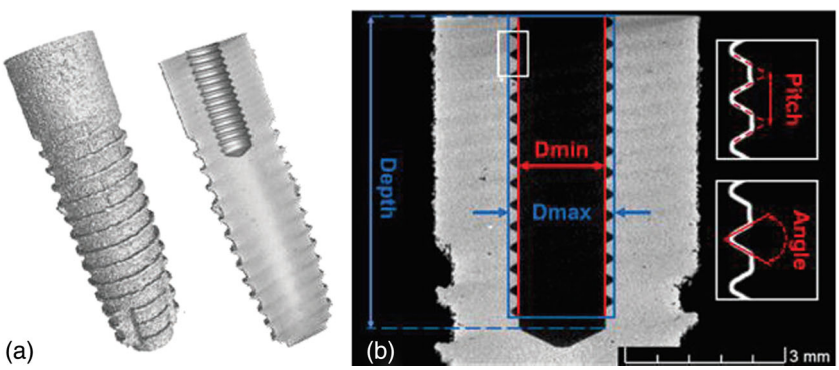

Fig. 35 **a** The Ti-6Al-4V dental pin produced by direct metal laser sintering (DMLS) after micro-drilling and **b** internal thread measured using X-ray computed tomography (CT) [129]

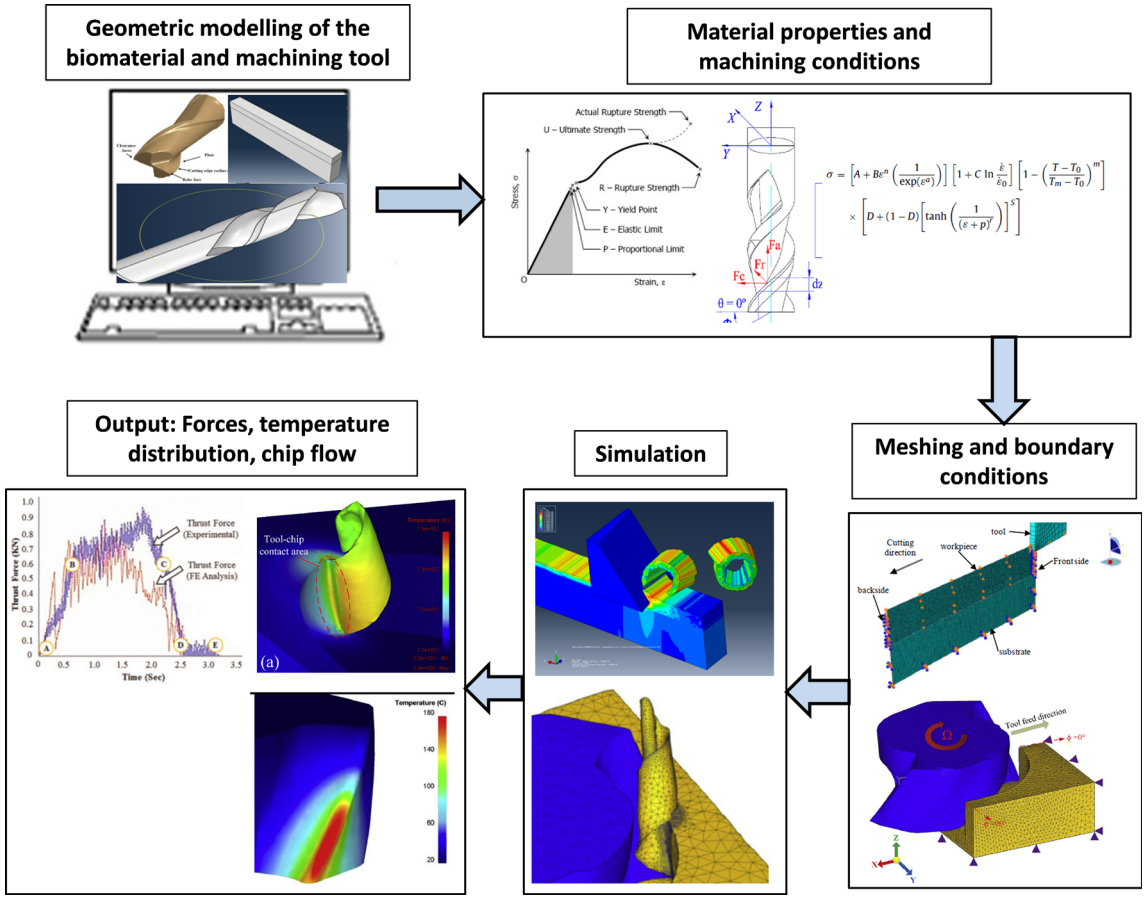

Fig. 36 Highlights of the general procedures of FEA modeling [127, 132]

chip thickness at the highest value), heat is diffused along a higher tool–workpiece contact length when maximum cutting speed the heat flows through a limited contact region.

In other work, finite element analysis of the orthogonal cutting Ti-6Al-4V using a 2D plane strain model was developed [134]. The focus of their research is mainly in the effects of the constitutive model and the chip separation criterion used in the finite element model on the forces, chip morphologies, and chip formation. An experimental orthogonal cutting setup for Ti-6Al-4V on a milling machine is presented as a benchmark to validate the models. Cutting conditions used in this research were cutting speed 30 m/min; depths of cut 40,

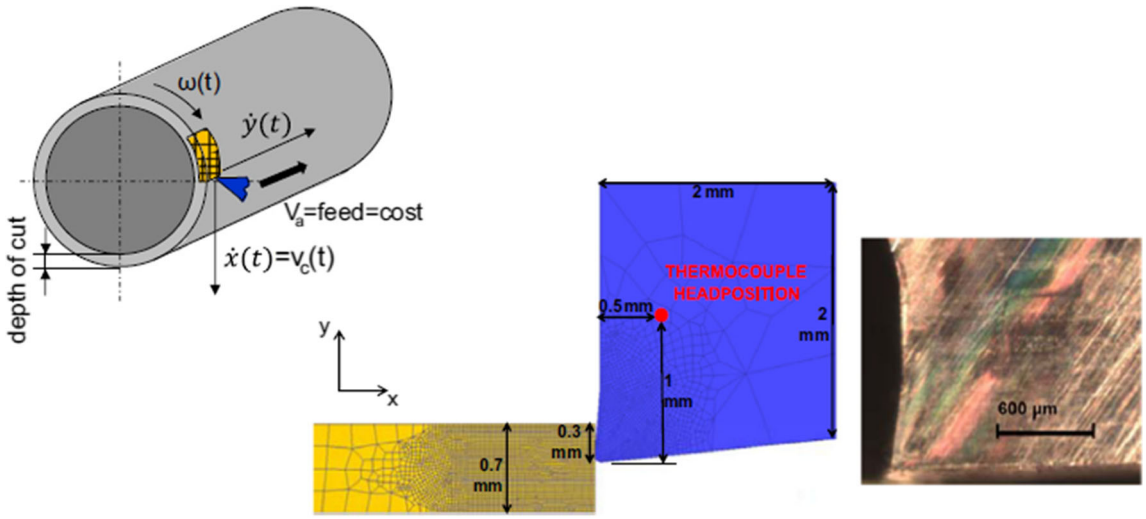

Fig. 37 Tool and workpiece modeling and the detail of tool micrograph used in the simulation of Ti-6Al-4V turning [133]

60, 100, and 280 μm; width of cut 1 mm; and length of cut 10 mm. The tool material is tungsten carbide with rake angle 15°; clearance angle 2°; and cutting edge radius 20 μm. From the experimental work, it was observed that there were two types of chip morphology: quasi-continuous for depth of cut 100, 60, and 40 μm and saw-toothed for 280 μm. Initially, the model was validated with the experiment for the depth of cut of 280 μm. The numerical cutting force is seen to be 40% lower than the experimental reference value and the chip morphology is seen to have shorter teeth. Therefore, the material constitutive model used in this research (the hyperbolic tangent (TANH) model) was modified by doubling the parameter value affecting the stress level. The forces value was improved; however, the chip formation mechanism is somehow diverged from the experimental results. Furthermore, the level of forces was not much affected by modifying the chip separation criterion when the chip separation criterion increases of about 10% of the tensile curve. In contrast, the feed force was significantly overestimated by the model. Figure 38 shows the comparison of the chip morphologies between the simulations (a–c) and experiments (d–f) for the depths of cut 100, 60, and 40 μm. In all three depths of cut, the model has chip morphology close to the experiments. The discrepancy may occur due to the selection of the chip separation criterion. It can be concluded that cutting forces are mainly affected by constitutive model while chip morphology is mainly controlled by chip separation criterion.

In addition, the selection of the toolpath and optimum process parameters in the micro-milling of Ti-6Al-4V alloys have also been studied [135]. These selections are important in order to avoid severe burr formation and rapid tool wear which can create significant problems such as poor surface roughness. In this study, mathematical model for achieving optimum process parameters and toolpath strategy was built based on the two-dimensional (2D) FE simulations and experimental results. The FE simulations were conducted to generate cutting forces and tool wear data whereas the initial micro-milling experiment was conducted to determine burr formation and surface roughness. Three main process parameters were considered for making the model, namely spindle speed, feed per tooth, and axial depth of cut. Subsequently, the multi objective optimization (MOPSO) is used to select the optimum parameters by four different approaches which considered the predictive models developed for cutting forces, tool wear depth, top-burr width, and surface roughness. The best model is achieved when the tool wear and cutting forces were considered as process constraints in the model. In order to achieve the optimum toolpath strategy, micro-milling experiment was conducted by producing circular thin ribs with thickness of 75 μm and height of 500 μm in a block of Ti-6Al-4V as shown in Fig. 39. The micro-end mills used in the experiments had two flutes, a 30° helix angle, a diameter of 508 μm, and a cutting length of 762 μm. It is found that tool wear is strongly affected by toolpath strategy and spindle speed or cutting speed while burr formation is significantly affected by toolpath strategy and axial depth of cut.

A 3D finite element modeling and simulation of micro-milling Ti-6Al-4V have been conducted by Thepsonthi and Özel [132]. The developed 3D finite element analysis is conducted to study forces, cutting temperature, tool wear rate, chip flow, and burr formation as an effect of the tool wear. Even though the simulation results such as forces and tool wear produced by 3D finite element can also be achieved by 2D finite element; however, the 3D model can show more realistic chip formation process (Fig. 40). It is suggested that down milling strategy has lower tool wear rate compared to up milling due to the cutting mechanisms during the tool enter the workpiece.

4.3 CNC precision multi-axis machining strategies for grinding and polishing

Computerized numerical control (CNC) precision machining is highly sought applications of machining to tailor the surface patterns of biomaterials so that it can improve the implant interaction and osseointegration with the biological tissue. For example, Holthaus et al. [136] produced a controlled patterns of micro U-shaped and V-shaped topography on hydroxypattite and zirconia biomaterials surfaces to improve their surface roughness. In order to machine components of high complex with partly free form surfaces such as knee implants, there is a need to use five or more axis machine tool and tool path strategies as shown in Fig. 41. For the required finishing surfaces of the knee implant, Denkena et al. [137] applied a two-step machining process using the multi-axis machining center. This combination of grinding as shown in Fig. 41a and polishing steps shown in Fig. 41b was managed to achieve the accuracy and surface quality of the mating knee implant surfaces.

Multi-axis CNC high-speed machining (HSM) [138] integrated with computer-aided design/computer-aided manufacturing (CAD/CAM) systems has also demonstrated a high-performance machining parameters. Apart from the minimized heat generation on the machined part, HSM has been found to be an excellent machining techniques for biomaterials such as titanium alloys in terms of high surface finish, less burr on the edges of the parts, and virtually stress-free components due to the low cutting forces involved [139]. On the other hand, Ritzberger et al. [140] applied a CAD/AM system to produce a Leucite-based glass-ceramics ($K[AlSi_2O_6]$), lithium disilicate-based glass-ceramics, and yttrium-stabilized zirconium oxide-based ceramic for precision dental restoration purposes. The process has three steps in which the first step is to scan the teeth with camera that should be interfaced with computer for the digital image analysis or image reconstruction. This can be done using specific

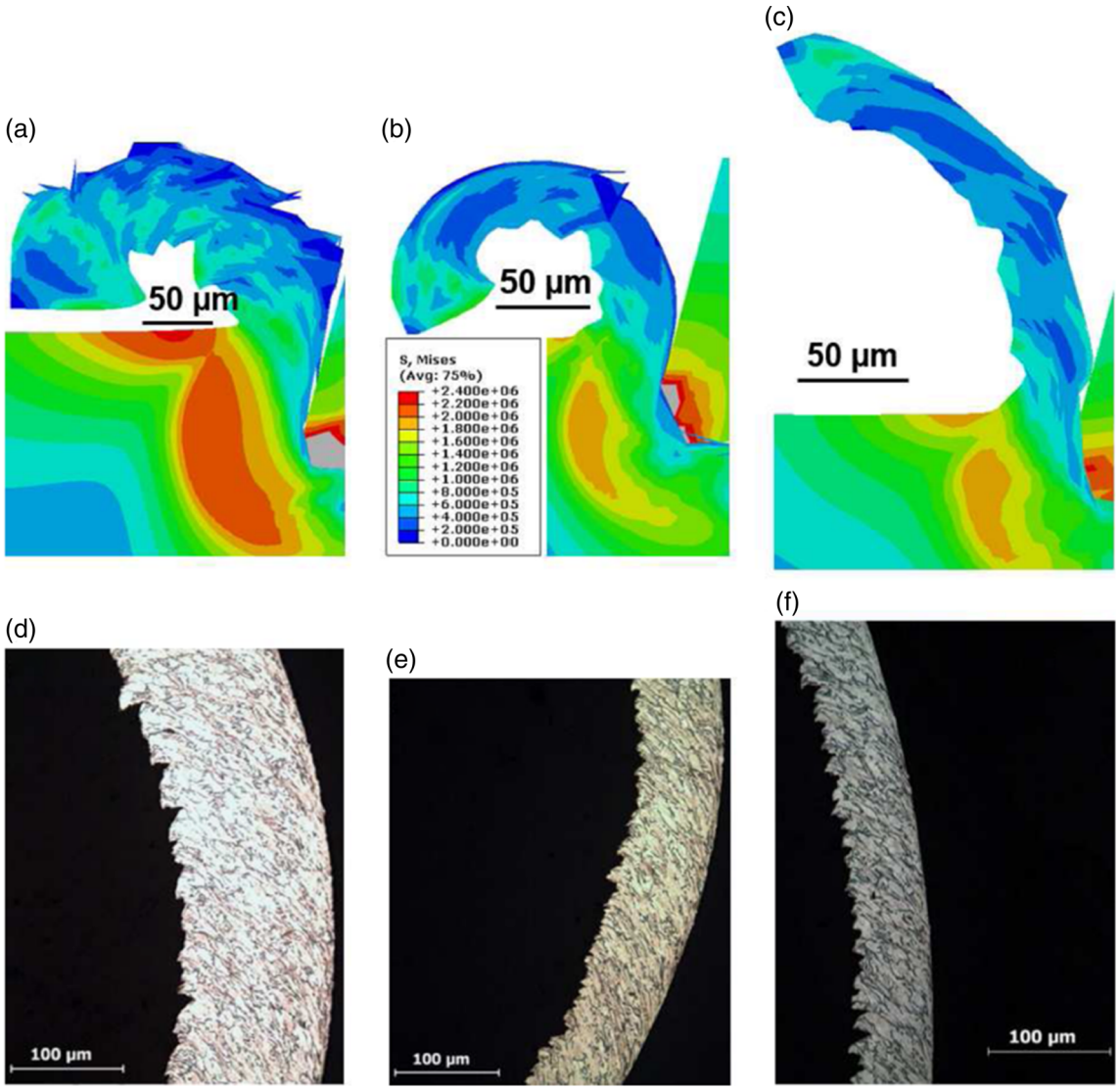

Fig. 38 Comparison of chip morphologies (Von Mises stress contours (e^3 Pa) from simulations and experimental at cutting speed of 30 m/min and depth of cut of **a**, **d** 100 mm, **b**, **e** 60 mm, and **c**, **f** 40 mm [134]

software for further modification or better design. Then having the virtual image, a manufacturing data (CAM) would be transmitted to the multi-axis CNC milling so that the required teeth with appropriate shape will be produced or constructed.

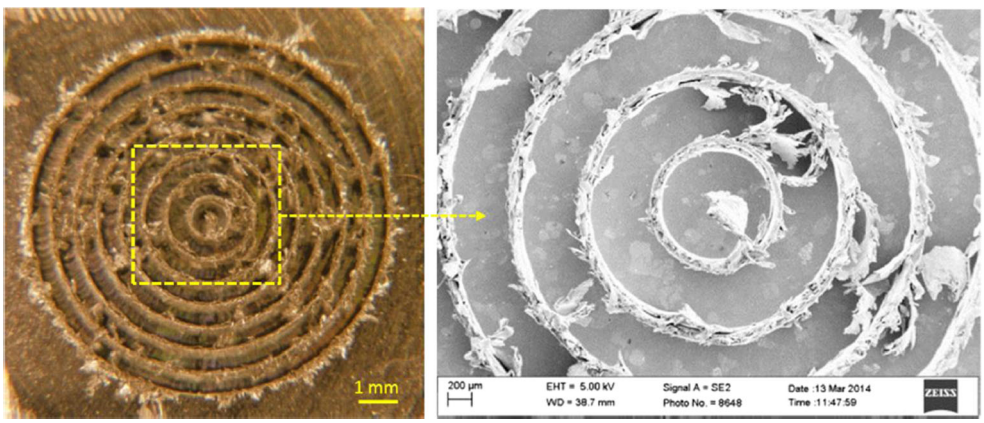

Fig. 39 The micro-milling result using the toolpath strategy of five z-levels (axial depth of cut = 90 μm), sixth z-level (axial depth of cut = 50 μm), and micro-milling parameters with spindle speed 16,000 rpm and feed per tooth 4.2 μm/tooth [135]

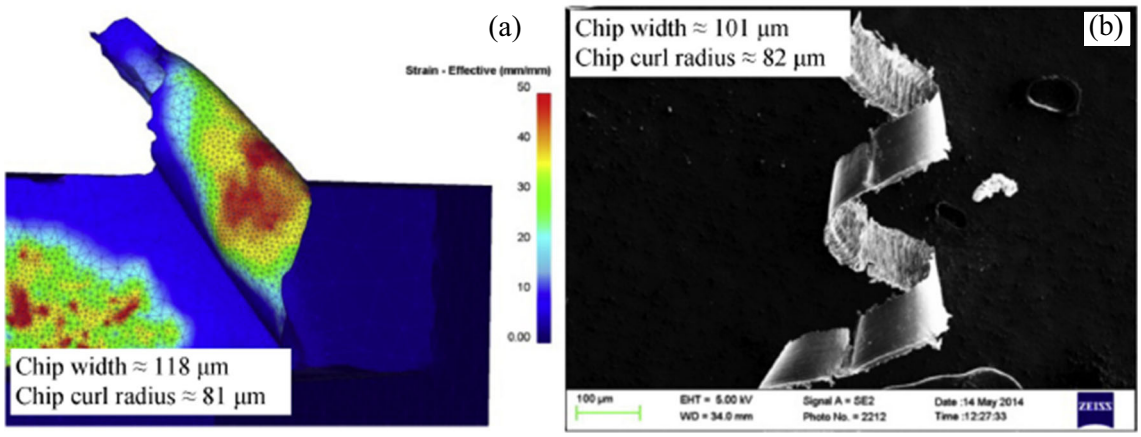

Fig. 40 Chip formation produced based on **a** 3D finite element model and **b** experimental work in micro-milling of Ti-6Al-4V [132]

Figure 42 shows the various CAD/CAM systems that can be applied in the production of biomaterial implants of such teeth. The system was found to be promising in the application of fabrication of crowns, fixed partial dentures, and other fields of dentistry and prosthetic devices which provided a state of art contribution to the health of human kind [141].

4.4 Additive manufacturing

On the other hand, the application of additive manufacturing (AM) often called the 3D printing has becoming attractive in healthcare industry due to its flexibility and powerful production technique. Some bio-implants have complex and small shapes that are difficult to be produced by using conventional or advanced machining processes. By utilizing the 3D printing technology, the route for implants production can be shorter and faster compared to the conventional route. This can be realized mainly due to the absence of rough machining process. Hence, additive manufacturing is more favorable to be used in the production of implants. In addition, the advancement of 3D scan technology also expedites the reverse engineering process in order to duplicate the needed implant shape especially for costume implants. Figure 43, schematically, shows the difference between conventional and advanced routes for the production of implants.

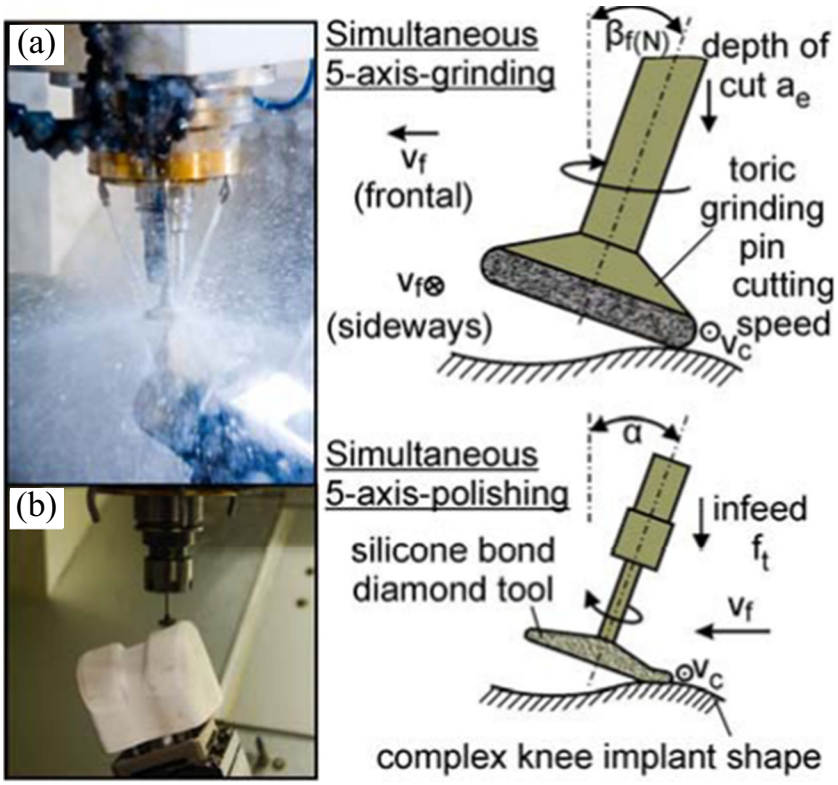

Fig. 41 Principle of five-axis machining of knee complex shape implants, **a** simultaneous five-axis grinding and **b** simultaneous five-axis polishing [137]

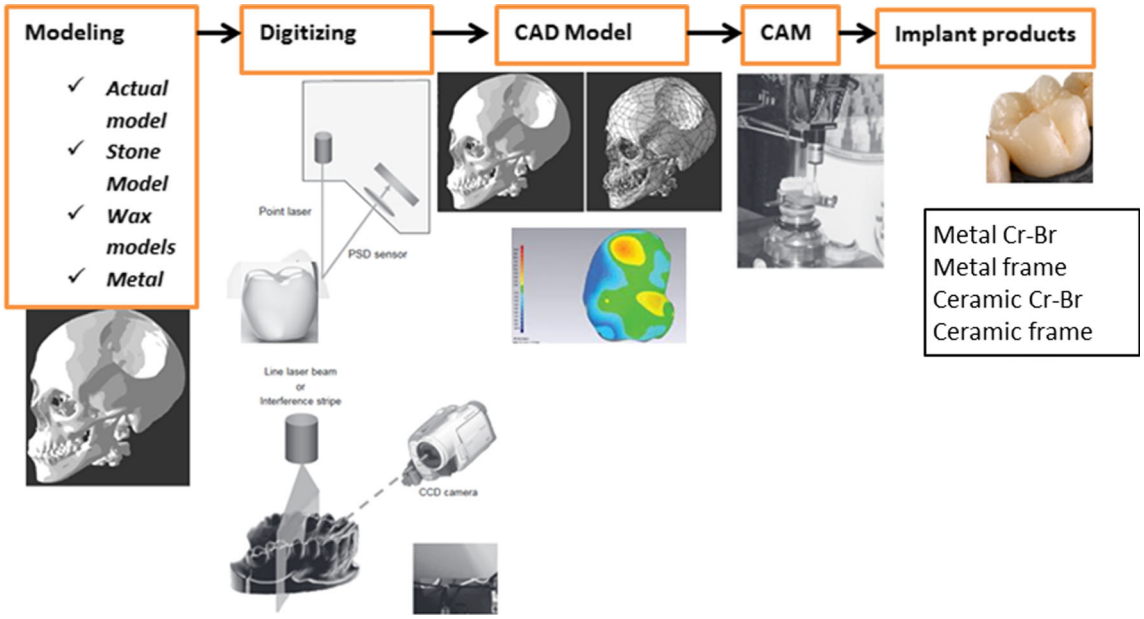

Fig. 42 CAD/CAM system in implant machining of various materials

3D printing is a proper name to describe the technologies that create 3D structures by adding layer by layer of materials. The materials can be ceramic, metal, and polymers (synthetic or natural polymers). The 3D printing technologies are commonly used by the computer, 3D modeling software (computer-aided design (CAD) or computer tomography (CT) scan images), machine equipment, and layering materials. After CAD sketch, 3D printing equipment reads out data from the CAD file and then 3D structure is produced [142, 143]. Out of the various types of AM technologies, the powder-based fusion which includes electron beam melting (EBM), selective laser sintering (SLS), and selective heat sintering (SHS) are the most widely used applications for metallic and ceramics biomaterials production. The processes use the CAD model of the part to produce a solid part by melting metallic powders layer by layer using electron beam or laser. Figure 44 shows the basic process processes of EBM and SLS in which it uses .STL data (triangulated model) of the part to be fabricated. The .STL model of the part is sliced into different layers, with each contoured layered data passed onto the system. Parts are built through a layer by layer process by directed solidification of the metal powder.

A controlled porous sizing and design of mechanical properties which meets the requirements of anatomy and functions at the vicinity of the implant was managed by electron beam melting (EBM). Hinel et al. [145] and Parthasarathy et al. [144] used the selective electron beam melting (SEBM) to develop novel cellular Ti-6Al-4V structures for orthopedic applications. This biomedical implant was found to be structurally superior in terms of mechanical properties such as hardness and tensile strength. Moreover, the future development of 3D printing or additive manufacturing is the use of different materials for the development of multi-material structures which can give a synergic advantage that cannot be obtained from a monolithic structure of biomaterial [143, 146]. Terrazas et al. [146] developed a sequence of production process to fabricate multi-material structure of Ti-6Al-4V and copper using electron beam melting (EBM). Even though AM

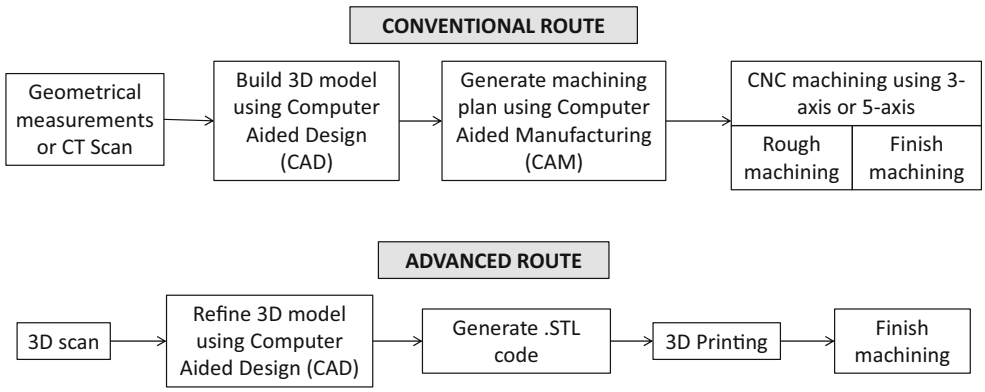

Fig. 43 Comparison of the production route for implants using conventional and advanced manufacturing methods

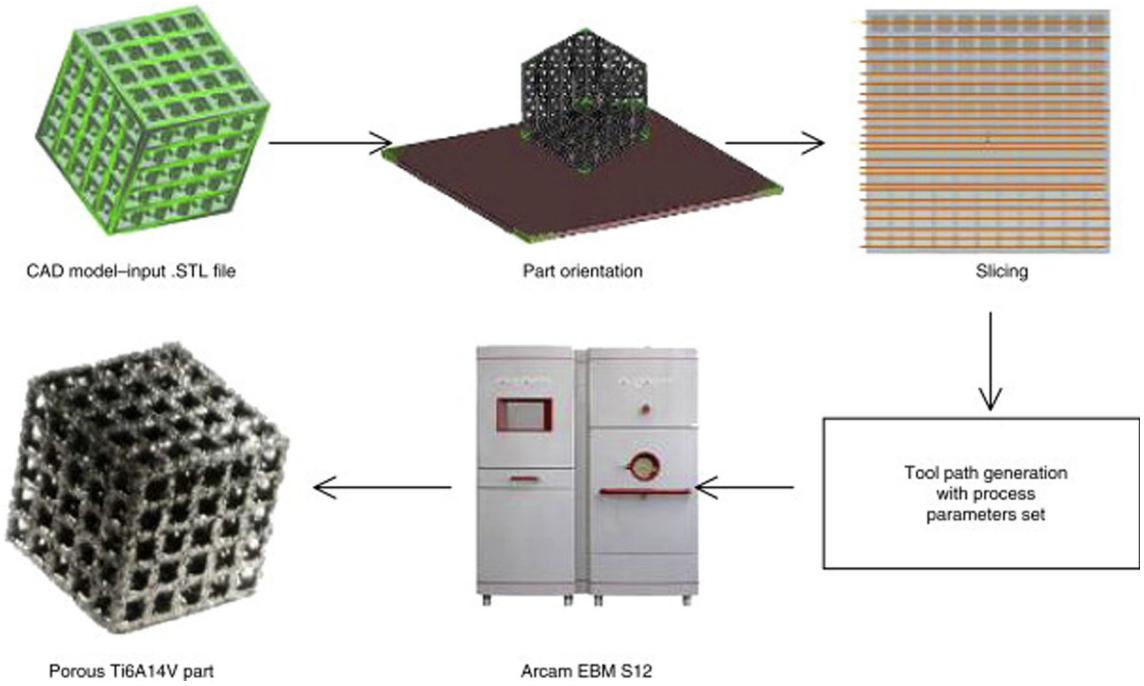

Fig. 44 Processing steps of electron beam melting (EBM) [144]

has a full-fledged prospect in the development of free form complex structures due to the layer by layer processing and certain directional grain growth, the mechanical properties of the printed biomaterial are not uniform along the line (anisotropy). This may create unpredictable material property or microstructural non-uniformity in the printed biomaterials. In order to reduce the unfavorable AM-produced biomaterial properties due to anisotropy, Zhang et al. [147] proposed a viewpoint of the application of topology optimization techniques in order to design or predict a reduced material weight and optimal performance parameters. The use of advanced material modeling, robust optimization algorithm development, and integration of process modeling to the structure optimization were some of the proposed techniques that can be used to reduce the challenges of additive manufacturing processing technology.

4.5 Hybrid processes

In recent years, due to the need for production of free form complex shape parts, improved surface finish, dimensional accuracy, and longer tool life, machine tool researchers are looking for a hybrid processing of biomaterials which is possible by combining several processes in one set up [148, 149]. In order to achieve these hybrid processes, a process planning algorithm is needed to be developed. The process planning algorithms shall be compatible with the simultaneous and controlled interaction of process mechanisms which may be based on the tools with the integrated machine. For example, Zhu et al. [149] developed a planning algorithm that able to simultaneously manage the hybrid processing of additive (fused filament fabrication, subtractive (CNC machining) and inspection activities) which resulted in a dimensional accuracy of the desired level. The results in terms of flexibility and capability were better than the individual additive and CNC machining processes.

A novel approach of hybrid machining which combined electric discharge machining and diamond abrasive grinding into a single process was successfully built for machining polycrystalline silicon materials [150]. Compared to the individual processes, the hybrid process can be used for biomaterials to increase shape accuracy, improve cylindricity, reduce damage-layer thickness of machined surfaces, and improve the surface roughness. Similarly, the performance of ultrasonic-assisted EDM, powder mixed-EDM, and powder mixed-ultrasonic-assisted EDM on Ti-6Al-4V titanium alloy was investigated to observe the effect of the hybrid process on the surface integrity such as surface roughness, micro cracks, heat-altered metal zone, and residual stress [151]. Based on the scanning electron microscopy (SEM) micrographs, it was concluded that all the investigated hybrid processes have better quality than the traditional EDM [151]. The process of dental restorations made from glass-ceramics was also improved by developing an ultrasonic vibration-assisted high-speed rotary cutting [152]. This hybrid machining setup helped the ceramic dental restoration process to be effective in a way that a reduced edge chipping and thus minimal subsurface damage was achieved. In developing an improved corrosion-resistant biodegradable magnesium–calcium (MgCa0.8 (wt.%) materials, Salahshoor et al. [37]

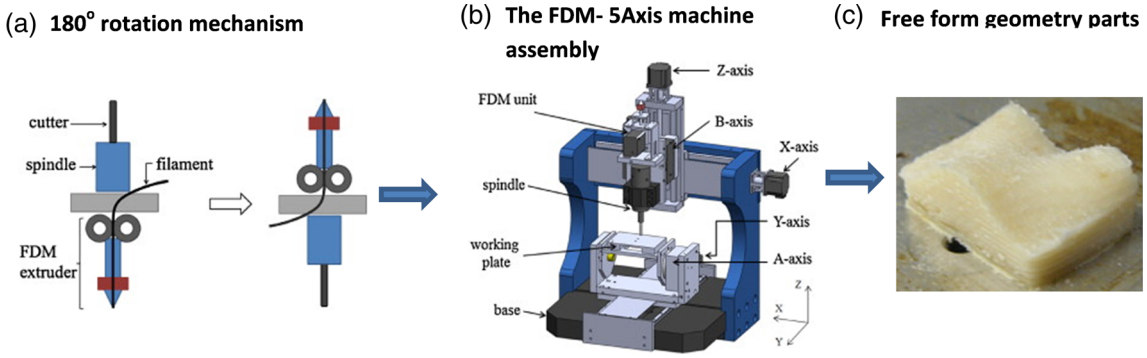

Fig. 45 **a**–**c** Hybrid processing of FDM and five-axis machining [153]

investigated the hybrid cutting-burnishing process on the surface integrity of the machined part. The experimental setup of the hybrid cutting-burnishing process was developed using a Cincinnati Arrow 500 CNC machine where polycrystalline diamond (PCD) inserts and silicon nitride ceramic ball was used for the end milling cutting and burnishing processes, respectively. The superior surface integrity (better surface finish) of the biomaterial was characterized by the high compressive hook-shaped residual stress profile, extended strain hardening, and little change of grain size in deep subsurface. Lee et al. [153] developed a hybrid rapid prototyping system which was designed by combining the fused deposition modeling (FDM) and five-axis machining. The basic concept was to synchronize the cutter spindle and the FDM extruder on a rotary axis of a desktop five-axis machine so that the opposite orientation of both cutting and layering operations will be alternatively engaged in 180° axis rotation as shown in Fig. 45a. It was demonstrated that the hybrid system can apparently produce better surface finish of freeform geometries as shown in Fig. 45c.

Hybridization of AM technologies is also the future works of machine tool industries where they integrated with multi-axis CNC machining processes for productivity improvement. In order to improve the 3D printing process in terms of the surface quality, the production cycle time and to process it in a "Done-in-One" mode, a hybrid multitasking machine tool has

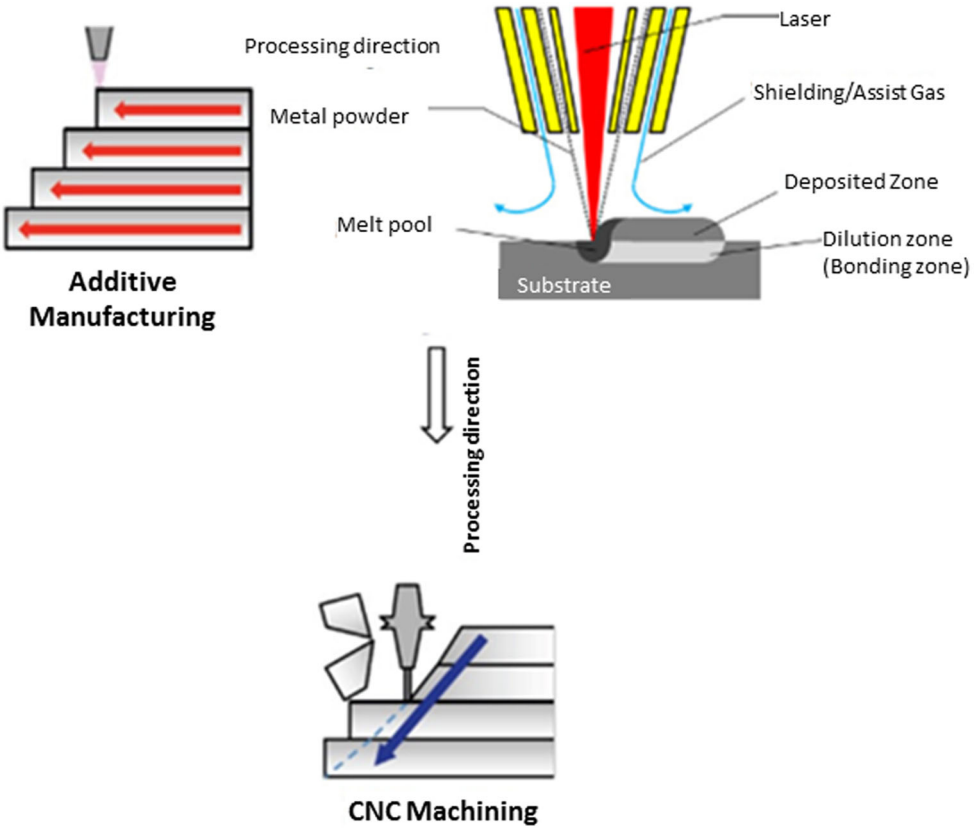

Fig. 46 Concept of hybridizing AM and CNC machining [154]

been developed by equipping laser metal deposition functionality in addition to existing integrated turning and milling capabilities [154]. In this equipment, the nearly net shape of biomaterials components is produced through AM and subsequently the finishing operations are conducted to achieve an accurate part finishing. The hybrid concept shown in Fig. 46, which is developed by Mazak machine tool industry, is based on the laser metal deposition (LMD) which is one of AM methods, is integrated with multi-axis CNC machine. In the LMD process, the part is produced layer by layer when the metal powder is melted on the substrate pool where by a fusion bond is formed.

Hybridization was also realized [155] through the development of additive/subtractive hybrid (A/SM) manufacturing process. In this technology, the additive and subtractive operations are executed alternatively that after a new layer is sintered (melted) and form a shape, the milling process follows until the final shape is produced. An experimental study on 18Ni(300) maraging steel powder was done and a better geometrical accuracies and improved mechanical properties were obtained when compared to the normal SLM process. In conclusion, in order to fully realize the application of these hybrid technologies, future works in developing a computer-aided process planning (CAPP), controller reconfigurations and online process monitoring are recommended [156].

5 Conclusion

The investigation on conventional and advanced machining of biocompatible materials has demonstrated the potential to produce a variety of biocompatible material specifications which can be used as implants. These machining processes can improve the quality of machined biocompatible materials and at the end produce implants of complex shape from metals, polymers, ceramics, and composites. The various machining techniques have an effect on the physical properties of the implants which may have a significant influence on the biocompatibility. This paper has highlighted that the machining parameters such as cutting speed, feed rate, and additional coolant have significant effects to the machined quality in the conventional machining process. Controlling these parameters and achieving optimum parameters can solve many challenges related with machining biocompatible materials. Due to the nature of most biocompatible materials, development of the advanced machining techniques has also been explored and discussed in order to complement the conventional machining process. The challenges for smaller size and future prospects of micro-scale machining of biomedical components using mechanical material removal process such as micro-milling have also investigated and reported. This paper has highlighted the prospects of process simulation and modeling in understanding and predicting the behavior of biomaterials during machining process using finite element analysis (FEA). Finally, due to the challenging need for complex shapes, tighter accuracy and lower surface finish of biocompatible materials advanced multi-axis CNC machining, additive manufacturing, and hybrid machining process can be applied to improve the quality and biocompatibility of a range of biomaterials.

Funding This research was supported by research grant RDU150121 from Ministry of Higher Education of Malaysia and Universiti Malaysia Pahang, Malaysia.

References

1. Mitsuishi M, Cao J, Bartolo P, Friedrich D, Shih AJ, Rajurkar K, Sugita N, Harada K (2013) Biomanufacturing. CIRP Ann Manuf Technol 62:585–606
2. Khan W, Muntimadugu E, Jaffe M, Domb AJ (2014) "Implantable medical devices."In: Focal controlled drug delivery: Springer, pp. 33–59
3. Bartolo P, Kruth J-P, Silva J, Levy G, Malshe A, Rajurkar K, Mitsuishi M, Ciurana J, Leu M (2012) Biomedical production of implants by additive electro-chemical and physical processes. CIRP Ann Manuf Technol 61:635–655
4. Kumar N, Arora NC, Datta B (2014) Bearing surfaces in hip replacement—evolution and likely future. Med J Armed Forces India 70:371–376
5. Meftah M, Klingenstein GG, Yun RJ, Ranawat AS, Ranawat CS (2013) Long-term performance of ceramic and metal femoral heads on conventional polyethylene in young and active patients: a matched-pair analysis. JBJS 95:1193–1197
6. Denkena B, Lucas A (2007) Biocompatible magnesium alloys as absorbable implant materials adjusted surface and subsurface properties by machining processes. CIRP Ann Manuf Technol 56:113–116
7. Meagher P, O'Cearbhaill ED, Byrne JH, Browne DJ (2016) Bulk metallic glasses for implantable medical devices and surgical tools. Adv Mater 28:5755–5762
8. Li HF, Zheng YF (2016) Recent advances in bulk metallic glasses for biomedical applications. Acta Biomater 36:1–20
9. Dambatta MS, Izman S, Yahaya B, Lim JY, Kurniawan D (2015) Mg-based bulk metallic glasses for biodegradable implant materials: a review on glass forming ability, mechanical properties, and biocompatibility. J Non-Cryst Solids 426:110–115
10. Abellán-Nebot JV, Siller HR, Vila C, Rodríguez CA (2012) An experimental study of process variables in turning operations of Ti–6Al–4V and Cr–Co spherical prostheses. Int J Adv Manuf Technol 63:887–902
11. Maji PK, Banerjee AJ, Banerjee PS, Karmakar S (2014) Additive manufacturing in prosthesis development—a case study. Rapid Prototyp J 20:480–489
12. Demir AG, Previtali B, Ge Q, Vedani M, Wu W, Migliavacca F, Petrini L, Biffi CA, Bestetti M (2014) Biodegradable magnesium coronary stents: material, design and fabrication. Int J Comput Integr Manuf 27:936–945

13. Kuczmaszewski J, Zagarski I, Zgarniak P (2016) Thermographic study of chip temperature in high-speed dry milling magnesium alloys. Manag Prod Eng Rev 7:86–92
14. Chen Y, Xu Z, Smith C, Sankar J (2014) Recent advances on the development of magnesium alloys for biodegradable implants. Acta Biomater 10:4561–4573
15. Sun S, Brandt M, Palanisamy S, Dargusch MS (2015) Effect of cryogenic compressed air on the evolution of cutting force and tool wear during machining of Ti-6Al-4V alloy. J Mater Process Technol 221:243–254
16. Kaynak Y, Karaca HE, Noebe RD, Jawahir IS (2013) Tool-wear analysis in cryogenic machining of NiTi shape memory alloys: a comparison of tool-wear performance with dry and MQL machining. Wear 306:51–63
17. Krishnamurthy G, Bhowmick S, Altenhof W, Alpas AT (2017) Increasing efficiency of Ti-alloy machining by cryogenic cooling and using ethanol in MRF. CIRP J Manuf Sci Technol 18:159–172
18. Niinomi M (2008) Mechanical biocompatibilities of titanium alloys for biomedical applications. J Mech Behav Biomed Mater 1: 30–42
19. Pfeifer R, Müller CW, Hurschler C, Kaierle S, Wesling V, Haferkamp H (2013) Adaptable orthopedic shape memory implants. Procedia CIRP 5:253–258
20. Tarniță D, Tarniță D, Bîzdoacă N, Mîndrilă I, Vasilescu M (2009) Properties and medical applications of shape memory alloys. Romanian J Morphol Embryol 50:15–21
21. Bakkal M, Shih AJ, Scattergood RO, Liu CT (2004) Machining of a ZrTiAlCuNi metallic glass. Scr Mater 50:583–588
22. Tönshoff HK, Winkler J (1997) The influence of tool coatings in machining of magnesium. Surf Coat Technol 94-95:610–616
23. Pramanik A (2014) Problems and solutions in machining of titanium alloys. Int J Adv Manuf Technol 70:919–928
24. Gao Y, Wang G, Liu B (2016) Chip formation characteristics in the machining of titanium alloys: a review. Int J Mach Mach Mater 18:155–184
25. Weinert K, Petzoldt V (2008) Machining NiTi micro-parts by micro-milling. Mater Sci Eng A 481-482:672–675
26. Piquard R, D'Acunto A, Laheurte P, Dudzinski D (2014) Micro-end milling of NiTi biomedical alloys, burr formation and phase transformation. Precis Eng 38:356–364
27. Li A, Zhao J, Zhou Y, Chen X, Wang D (2012) Experimental investigation on chip morphologies in high-speed dry milling of titanium alloy Ti-6Al-4V. Int J Adv Manuf Technol 62:933–942
28. Özel T, Thepsonthi T, Ulutan D, Kaftanoğlu B (2011) Experiments and finite element simulations on micro-milling of Ti–6Al–4V alloy with uncoated and cBN coated micro-tools. CIRP Ann 60:85–88
29. Cellier A, Chalon F, Grimal-Perrigouas V, Bonhoure D, Leroy R (2014) Effects of cutting angles in Ti-6al-4v milling process on surface integrity: influence of roughness and residual stresses on fatigue limit. Mach Sci Technol 18:565–584
30. Bakkal M, Shih AJ, Scattergood RO (2004) Chip formation, cutting forces, and tool wear in turning of Zr-based bulk metallic glass. Int J Mach Tools Manuf 44:915–925
31. Bakkal M, Nakay ler V (2009) Cutting mechanics of bulk metallic glass materials on meso-end milling. Mater Manuf Process 24: 1249–1255
32. Bakkal M, Liu CT, Watkins TR, Scattergood RO, Shih AJ (2004) Oxidation and crystallization of Zr-based bulk metallic glass due to machining. Intermetallics 12:195–204
33. Shaw MC (1984) Metal cutting principles, 3 ed. Oxford University Press, Oxford
34. Bílek O, Javořík J, Lukovics I (2015) Manufacturing technology of prosthetic parts: 3-axis CNC milling of master model. Int J Mech
35. Dhokia V, Bilzon J, Seminati E, Talamas DC, Young M, Mitchell W (2017) The design and manufacture of a prototype personalized liner for lower limb amputees. Procedia CIRP 60:476–481
36. Shi K, Zhang D, Ren J (2015) Optimization of process parameters for surface roughness and microhardness in dry milling of magnesium alloy using Taguchi with grey relational analysis. Int J Adv Manuf Technol 81:645–651
37. Salahshoor M, Li C, Liu ZY, Fang XY, Guo YB (2018) Surface integrity and corrosion performance of biomedical magnesium-calcium alloy processed by hybrid dry cutting-finish burnishing. J Mech Behav Biomed Mater 78:246–253
38. Wang F, Zhao J, Li A, Zhao J (2014) Experimental study on cutting forces and surface integrity in high-speed side milling of Ti-6Al-4V titanium alloy. Mach Sci Technol 18:448–463
39. García-Barbosa JA, Arroyo-Osorio JM, Córdoba-Nieto E (2017) Influence of tool inclination on chip formation process and roughness response in ball-end milling of freeform surfaces on Ti-6Al-4V alloy. Mach Sci Technol 21:121–135
40. Sutter G, List G (2013) Very high speed cutting of Ti6Al4V titanium alloy change in morphology and mechanism of chip formation. Int J Mach Tools Manuf 66:37–43
41. Han D, Wang G, Li J, Chan K, S. To, Wu F, Gao Y, Zhai Q (2015) Cutting characteristics of Zr-based bulk metallic glass. J Mater Sci Technol 31:153–158
42. Sunil BR, Ganesh KV, Pavan P, Vadapalli G, Swarnalatha C, Swapna P, Bindukumar P, Reddy GPK (2016) Effect of aluminum content on machining characteristics of AZ31 and AZ91 magnesium alloys during drilling. J Magnesium Alloys 4:15–21
43. Schwieger K, Carrero V, Rentzsch R, Becker A, Bishop N, Hille E, Louis H, Morlock M, Honl M (2004) Abrasive water jet cutting as a new procedure for cutting cancellous bone—in vitro testing in comparison with the oscillating saw. J Biomed Mater Res B Appl Biomater 71B:223–228
44. den Dunnen S, Kraaij G, Biskup C, Kerkhoffs GMMJ, Tuijthof GJM (2013) Pure waterjet drilling of articular bone: an in vitro feasibility study. Stroj Vestn J Mech Eng 59:425–432
45. den Dunnen S, Mulder L, Kerkhoffs GM, Dankelman J, Tuijthof GJ (2013) Waterjet drilling in porcine bone: the effect of the nozzle diameter and bone architecture on the hole dimensions. J Mech Behav Biomed Mater 27:84–93
46. Wessels V, Grigoryev A, Dold C, Wyen C-F, Roth R, Weingärtner E, Pude F, Wegener K, Löffler JF (2012) Abrasive waterjet machining of three-dimensional structures from bulk metallic glasses and comparison with other techniques. J Mater Res 27:1187–1192
47. Shiou F-J, Loc PH, Dang NH (2013) Surface finish of bulk metallic glass using sequential abrasive jet polishing and annealing processes. Int J Adv Manuf Technol 66(1–11):1523–1533
48. Chillman A, Ramulu M, Hashish M (2007) Waterjet peening and surface preparation at 600 MPa: a preliminary experimental study. J Fluids Eng 129:485–490
49. Arola DD, McCain ML (2000) Abrasive waterjet peening: a new method of surface preparation for metal orthopedic implants. J Biomed Mater Res 53:536–546
50. Barriuso S, Lieblich M, Multigner M, Etxeberria I, Alberdi A, González-Carrasco JL (2011) Roughening of metallic biomaterials by abrasiveless waterjet peening: characterization and viability. Wear 270:634–639
51. Lieblich M, Barriuso S, Ibáñez J, Ruiz-de-Lara L, Díaz M, Ocaña JL, Alberdi A, González-Carrasco JL (2016) On the fatigue behavior of medical Ti6Al4V roughened by grit blasting and abrasiveless waterjet peening. J Mech Behav Biomed Mater 63: 390–398
52. Kong MC, Axinte D, Voice W (2011) Challenges in using waterjet machining of NiTi shape memory alloys: an analysis of controlled-depth milling. J Mater Process Technol 211:959–971

53. Kong MC, Srinivasu D, Axinte D, Voice W, McGourlay J, Hon B (2013) On geometrical accuracy and integrity of surfaces in multi-mode abrasive waterjet machining of NiTi shape memory alloys. CIRP Ann 62:555–558
54. Frotscher M, Kahleyss F, Simon T, Biermann D, Eggeler G (2011) Achieving small structures in thin NiTi sheets for medical applications with water jet and micro machining: a comparison. J Mater Eng Perform 20:776–782
55. Singh R, Khamba JS (2006) Ultrasonic machining of titanium and its alloys: a review. J Mater Process Technol 173:125–135
56. Choi Y-J, Park K-H, Hong Y-H, Kim K-T, Lee S-W, Choi H-Z (2013) Effect of ultrasonic vibration in grinding; horn design and experiment. Int J Precis Eng Manuf 14:1873–1879
57. Xiao X, Zheng K, Liao W (2014) Theoretical model for cutting force in rotary ultrasonic milling of dental zirconia ceramics. Int J Adv Manuf Technol 75:1263–1277
58. Zheng K, Li Z, Liao W, Xiao X (2017) Friction and wear performance on ultrasonic vibration assisted grinding dental zirconia ceramics against natural tooth. J Braz Soc Mech Sci Eng 39: 833–843
59. Sioshansi P, Tobin EJ (1996) Surface treatment of biomaterials by ion beam processes. Surf Coat Technol 83:175–182
60. He W, Poker DB, Gonsalves KE, Batina N (2003) Micro/nano machining of polymeric substrates by ion beam techniques. Microelectron Eng 65:153–161
61. Cui FZ, Luo ZS (1999) Biomaterials modification by ion-beam processing. Surf Coat Technol 112:278–285
62. Yin GF, Luo JM, Zheng CQ, Tong HH, Huo YF, Mu LL (1999) Preparation of DLC gradient biomaterials by means of plasma source ion implant-ion beam enhanced deposition. Thin Solid Films 345:67–70
63. Choi J-M, Kim H-E, Lee I-S (2000) Ion-beam-assisted deposition (IBAD) of hydroxyapatite coating layer on Ti-based metal substrate. Biomaterials 21:469–473
64. Park Y-S, Yi K-Y, Lee I-S, Han C-H, Jung Y-C (2005) The effects of ion beam-assisted deposition of hydroxyapatite on the grit-blasted surface of endosseous implants in rabbit tibiae. Int J Oral Maxillofac Implants:20
65. Ghany KA, Newishy M (2005) Cutting of 1.2 mm thick austenitic stainless steel sheet using pulsed and CW Nd: YAG laser. J Mater Process Technol 168:438–447
66. Erika G-L, Alexis M-T, Juansethi I-M, Alex E-Z, Ciro AR (2016) Fiber laser microcutting of AISI 316L stainless steel tubes-influence of pulse energy and spot overlap on back wall dross. Procedia CIRP 49:222–226
67. Sealy M, Guo Y, Liu J, Li C (2016) Pulsed laser cutting of magnesium-calcium for biodegradable stents. Procedia CIRP 42: 67–72
68. Almeida I, De Rossi W, Lima M, Berretta J, Nogueira G, Wetter N, Vieira N (2006) Optimization of titanium cutting by factorial analysis of the pulsed Nd: YAG laser parameters. J Mater Process Technol 179:105–110
69. Guerra AJ, Farjas J, Ciurana J (2017) Fibre laser cutting of polycaprolactone sheet for stents manufacturing: a feasibility study. Opt Laser Technol 95:113–123
70. Riveiro A, Soto R, Comesaña R, Boutinguiza M, Del Val J, Quintero F, Lusquiños F, Pou J (2012) Laser surface modification of PEEK. Appl Surf Sci 258:9437–9442
71. Riveiro A, Soto R, Del Val J, Comesaña R, Boutinguiza M, Quintero F, Lusquiños F, Pou J (2014) Laser surface modification of ultra-high-molecular-weight polyethylene (UHMWPE) for biomedical applications. Appl Surf Sci 302:236–242
72. Riveiro A, Soto R, del Val J, Comesaña R, Boutinguiza M, Quintero F, Lusquiños F, Pou J (2016) Texturing of polypropylene (PP) with nanosecond lasers. Appl Surf Sci 374:379–386
73. Fu C, Liu J, Guo A (2015) Statistical characteristics of surface integrity by fiber laser cutting of Nitinol vascular stents. Appl Surf Sci 353:291–299
74. Hung C-H, Chang F-Y, Chang T-L, Chang Y-T, Huang K-W, Liang P-C (2015) Micromachining NiTi tubes for use in medical devices by using a femtosecond laser. Opt Lasers Eng 66:34–40
75. Hung C-H, Chang F-Y (2017) Curve micromachining on the edges of nitinol biliary stent by ultrashort pulses laser. Opt Laser Technol 90:1–6
76. Ng C, Chan C, Man H, Waugh D, Lawrence J (2017) NiTi shape memory alloy with enhanced wear performance by laser selective area nitriding for orthopaedic applications. Surf Coat Technol 309: 1015–1022
77. Moura C, Pereira R, Buciumeanu M, Carvalho O, Bartolomeu F, Nascimento R, Silva F (2017) Effect of laser surface texturing on primary stability and surface properties of zirconia implants. Ceram Int 43:15227–15236
78. Sharma K, Kedia S, Singh A, Basak C, Chauhan A, Basu S, Sinha S (2016) Morphology and structural studies of laser treated 45S5 bioactive glass. J Non-Cryst Solids 440:43–48
79. Ntasi A, Mueller WD, Eliades G, Zinelis S (2010) The effect of electro discharge machining (EDM) on the corrosion resistance of dental alloys. Dent Mater 26:e237-e245
80. J. Strasky, M. Janecek, and P. Harcuba, "Electric discharge machining of Ti-6Al-4V alloy for biomedical use," 2011
81. Gu L, Li L, Zhao W, Rajurkar KP (2012) Electrical discharge machining of Ti6Al4V with a bundled electrode. Int J Mach Tools Manuf 53:100–106
82. Strasky J, Janecek M, Harcuba P (2011) Electric discharge machining of Ti-6Al-4V alloy for biomedical use. Proc Contrib Papers Part III(WDS'11):127–131
83. Otsuka F, Kataoka Y, Miyazaki T (2012) Enhanced osteoblast response to electrical discharge machining surface. Dent Mater J 31:309–315
84. Theisen W, Schuermann A (2004) Electro discharge machining of nickel-titanium shape memory alloys. Mater Sci Eng A 378:200–204
85. Klocke F, Schwade M, Klink A, Veselovac D, Kopp A (2013) Influence of electro discharge machining of biodegradable magnesium on the biocompatibility. Procedia CIRP 5:88–93
86. Klocke F, Schwade M, Kopp A (2012) "Concept for the machining of biodegradable magnesium by EDM in combination with electrochemical surface treatment," In: Proceedings of the 1st international conference on design and processes for medical devices
87. Huang H, Yan J (2015) On the surface characteristics of a Zr-based bulk metallic glass processed by microelectrical discharge machining. Appl Surf Sci 355:1306–1315
88. Bucciotti F, Mazzocchi M, Bellosi A (2010) Perspectives of the Si 3 N 4-TiN ceramic composite as a biomaterial and manufacturing of complex-shaped implantable devices by electrical discharge machining (EDM). J Appl Biomater Biomech 8
89. Park HW, Lee I (2014) Large pulsed electron beam surface treatment of translucent PMMA. Appl Surf Sci 308:311–315
90. Faltermeier A, Behr M, Reicheneder C, Proff P, Römer P (2011) Electron-beam irradiation of polymer bracket materials. Am J Orthod Dentofac Orthop 139:7–11
91. Han C-M, Lee E-J, Kim H-E, Koh Y-H, Kim KN, Ha Y, Kuh S-U (2010) The electron beam deposition of titanium on polyetheretherketone (PEEK) and the resulting enhanced biological properties. Biomaterials 31:3465–3470
92. Behr M, Rosentritt M, Faltermeier A, Handel G (2005) Electron beam irradiation of dental composites. Dent Mater 21:804–810
93. Folkes J (2009) Waterjet—an innovative tool for manufacturing. J Mater Process Technol 209:6181–6189

94. Azhari A, Schindler C, Kerscher E, Grad P (2012) Improving surface hardness of austenitic stainless steel using waterjet peening process. Int J Adv Manuf Technol 63:1035–1046
95. Syazwani H, Mebrahitom G, Azmir A (2016) A review on nozzle wear in abrasive water jet machining application. IOP Conf Ser Mater Sci Eng 114:012020
96. Kovacevic R, Hashish M, Mohan R, Ramulu M, Kim TJ, Geskin ES (1997) State of the art of Research and development in abrasive waterjet machining. J Manuf Sci Eng 119:776–785
97. Liu J-X, Yang D-Z, Shi F, Cai Y-J (2003) Sol–gel deposited TiO2 film on NiTi surgical alloy for biocompatibility improvement. Thin Solid Films 429:225–230
98. Azhari A, Schindler C, Godard C, Gibmeier J, Kerscher E (2016) Effect of multiple passes treatment in waterjet peening on fatigue performance. Appl Surf Sci 388, pp:468–474
99. Arola D, Alade AE, Weber W (2006) Improving fatigue strength of metals using abrasive waterjet peening. Mach Sci Technol 10: 197–218
100. Baleani M, Viceconti M, Toni A (2000) The effect of sandblasting treatment on endurance properties of titanium alloy hip prostheses. Artif Organs 24:296–299
101. Thoe TB, Aspinwall DK, Wise MLH (1998) Review on ultrasonic machining. Int J Mach Tools Manuf 38:239–255
102. Lv D, Huang Y, Wang H, Tang Y, Wu X (2013) Improvement effects of vibration on cutting force in rotary ultrasonic machining of BK7 glass. J Mater Process Technol 213:1548–1557
103. McGeough JA (1988) Advanced methods of machining: Springer Science & Business Media
104. Allen DM, Shore P, Evans RW, Fanara C, O'Brien W, Marson S, O'Neill W (2009) Ion beam, focused ion beam, and plasma discharge machining. CIRP Ann 58:647–662
105. Rautray TR, Narayanan R, Kim K-H (2011) Ion implantation of titanium based biomaterials. Prog Mater Sci 56:1137–1177
106. Meijer J (2004) Laser beam machining (LBM), state of the art and new opportunities. J Mater Process Technol 149:2–17
107. Majumdar JD, Manna I (2003) Laser processing of materials. Sadhana 28:495–562
108. Martin J, Schwartz Z, Hummert T, Schraub D, Simpson J, Lankford J, Dean D, Cochran D, Boyan B (1995) Effect of titanium surface roughness on proliferation, differentiation, and protein synthesis of human osteoblast-like cells (MG63). J Biomed Mater Res A 29:389–401
109. Okada A (2014) Electron beam machining. In: Laperrière L, Reinhart G (eds) CIRP Encyclopedia of Production Engineering. Springer Berlin Heidelberg, Berlin, Heidelberg, pp 446–452
110. Kim J, Lee WJ, Park HW (2016) The state of the art in the electron beam manufacturing processes. Int J Precis Eng Manuf 17:1575–1585
111. Kumar A, Hiremath SS (2016) Improvement of geometrical accuracy of micro holes machined through micro abrasive jet machining. Procedia CIRP 46:47–50
112. Grinspan AS, Gnanamoorthy R (2006) A novel surface modification technique for the introduction of compressive residual stress and preliminary studies on Al alloy AA6063. Surf Coat Technol 201:1768–1775
113. Dubey AK, Yadava V (2008) Laser beam machining—a review. Int J Mach Tools Manuf 48:609–628
114. Ding K, Ye L (2006) Simulation of multiple laser shock peening of a 35CD4 steel alloy. J Mater Process Technol 178:162–169
115. Huang H, Zheng HY, Liu Y (2005) Experimental investigations of the machinability of Ni 50.6 Ti 49.4 alloy. Smart Mater Struct 14: S297–S301
116. Lau WS, Lee WB (1991) A comparison between EDM wire-cut and laser cutting of carbon fibre composite materials. Mater Manuf Process 6:331–342
117. Kozak J, Rajurkar KP, Chandarana N (2004) Machining of low electrical conductive materials by wire electrical discharge machining (WEDM). J Mater Process Technol 149:266–271
118. Bae H, Chu H, Edalat F, Cha JM, Sant S, Kashyap A, Ahari AF, Kwon CH, Nichol JW, Manoucheri S, Zamanian B, Wang Y, Khademhosseini A (2014) Development of functional biomaterials with micro- and nanoscale technologies for tissue engineering and drug delivery applications. J Tissue Eng Regen Med 8:1–14
119. Okada A (2016) Electron beam machining. In: Laperrière L, Reinhart G (eds) CIRP Encyclopedia of Production Engineering, P. The international academy for. Springer Berlin Heidelberg, Berlin, Heidelberg, pp 1–6
120. An YH, Draughn RA (1999) Mechanical testing of bone and the bone-implant interface. CRC press
121. Knowles MRH, Rutterford G, Karnakis D, Ferguson A (May 01 2007) Micro-machining of metals, ceramics and polymers using nanosecond lasers. Int J Adv Manuf Technol 33:95–102
122. Hallgren C, Reimers H, Chakarov D, Gold J, Wennerberg A (2003) An in vivo study of bone response to implants topographically modified by laser micromachining. Biomaterials 24:701–710
123. Saptaji K (2015) Mechanical micro-machining. In: Nee AYC (ed) Handbook of manufacturing engineering and technology. Springer, London, pp 1089–1107
124. Attanasio A, Gelfi M, Pola A, Ceretti E, Giardini C (2013) Influence of material microstructures in micromilling of Ti6Al4V alloy. Materials 6:4268–4283
125. Saptaji K, Subbiah S, Dhupia JS (2012) Effect of side edge angle and effective rake angle on top burrs in micro-milling. Precis Eng 36:444–450
126. Saptaji K, Subbiah S (2017) Burr reduction of micro-milled microfluidic channels mould using a tapered tool. Procedia Eng 184:137–144
127. Kushendarsyah S, Sathyan S (2013) Orthogonal microcutting of thin workpieces. J Manuf Sci Eng 135:031004
128. Ervine P, OaDonnell GE, Walsh B (2015) Fundamental investigations into burr formation and damage mechanisms in the micromilling of a biomedical grade polymer. Mach Sci Technol 19:112–133
129. Rysava Z, Bruschi S, Carmignato S, Medeossi F, Savio E, Zanini F (2016) Micro-drilling and threading of the Ti6Al4V titanium alloy produced through additive manufacturing. Procedia CIRP 46: 583–586
130. Mebrahitom A, Choon W, Azhari A (2017) Side milling machining simulation using finite element analysis: prediction of cutting forces. Mater Today Proc 4(4):5215–5221
131. Gebremariam MA, Xiang Yuan S, Azhari A, Lemma TA (2017) Remaining tool life prediction based on force sensors signal during end milling of Stavax ESR Steel. Adv Manuf 2: V002T02A094-C1
132. Thepsonthi T, Özel T (2015) 3-D finite element process simulation of micro-end milling Ti-6Al-4V titanium alloy: experimental validations on chip flow and tool wear. J Mater Process Technol 221: 128–145
133. Chiappini E, Tirelli S, Albertelli P, Strano M, Monno M (2014) On the mechanics of chip formation in Ti6Al4V turning with spindle speed variation. Int J Mach Tools Manuf 77:16–26
134. Ducobu F, Rivière-Lorphèvre E, Filippi E (2016) Material constitutive model and chip separation criterion influence on the modeling of Ti6Al4V machining with experimental validation in strictly orthogonal cutting condition. Int J Mech Sci 107:136–149
135. Thepsonthi T, A–zel T (2014) An integrated toolpath and process parameter optimization for high-performance micro-milling process of Tia6Ala4V titanium alloy. Int J Adv Manuf Technol 75: 57–75

136. Holthaus M g, Twardy S, Stolle J, Riemer O, Treccani L, Brinksmeier E, Rezwan K (2012) Micromachining of ceramic surfaces: hydroxyapatite and zirconia. J Mater Process Technol 212:614–624
137. Denkena B, Köhler J, Turger A, Helmecke P, Correa T, Hurschler C (2013) Manufacturing conditioned wear of all-ceramic knee prostheses. Procedia CIRP 5:179–184
138. Mebrahitom A, Rizuan D, Azmir M, Nassif M (2016) Effect of high-speed milling tool path strategies on the surface roughness of Stavax ESR mold insert machining. IOP Conf Ser Mater Sci Eng 114:012006
139. Rahman M, Wang Z-G, Wong Y-S (2006) A review on high-speed machining of titanium alloys. JSME Int J Ser C Mech Syst Mach Elem Manuf 49:11–20
140. Ritzberger C, Apel E, Höland W, Peschke A, Rheinberger V (2010) Properties and clinical application of three types of dental glass-ceramics and ceramics for CAD-CAM Technologies. Materials 3:3700–3713
141. Miyazaki T, Hotta Y, Kunii J, Kuriyama S, Tamaki Y (2009) A review of dental CAD/CAM: current status and future perspectives from 20 years of experience. Dent Mater J:44–56
142. Gu BK, Choi DJ, Park SJ, Kim MS, Kang CM, Kim C-H (2016) 3-dimensional bioprinting for tissue engineering applications. *Biomaterials Research* 20:12
143. Bandyopadhyay A, Bose S, Das S (2015) 3D printing of biomaterials. MRS Bull 40:108–115
144. Parthasarathy J, Starly B, Raman S, Christensen A (2010) Mechanical evaluation of porous titanium (Ti6Al4V) structures with electron beam melting (EBM). J Mech Behav Biomed Mater 3:249–259
145. Heinl P, Maller L, Karner C, Singer RF, Maller FA (2008) Cellular Ti6Al4V structures with interconnected macro porosity for bone implants fabricated by selective electron beam melting. Acta Biomater 4:1536–1544
146. Terrazas CA, Gaytan SM, Rodriguez E, Espalin D, Murr LE, Medina F, Wicker RB (March 01 2014) Multi-material metallic structure fabrication using electron beam melting. Int J Adv Manuf Technol 71:33–45
147. Zhang P, Liu J, To AC (2017) Role of anisotropic properties on topology optimization of additive manufactured load bearing structures. Scr Mater 135:148–152
148. Chavoshi SZ, Luo X (2015) Hybrid micro-machining processes: a review. Precis Eng 41:1–23
149. Zhu Z, Dhokia V, Newman ST, Nassehi A (2014) Application of a hybrid process for high precision manufacture of difficult to machine prismatic parts. Int J Adv Manuf Technol 74:1115–1132
150. Zhou W, Liu Z, Zhang B, Qiu M, Chen H, Shen L (2018) Experimental research on semiconductor shaping by abrasive-spark hybrid machining. Int J Adv Manuf Technol 94:2209–2216
151. Khosrozadeh B, Shabgard M (2017) Effects of hybrid electrical discharge machining processes on surface integrity and residual stresses of Ti-6Al-4V titanium alloy. Int J Adv Manuf Technol 93:1999–2011
152. Song X-F, Yang J-J, Ren H-T, Lin B, Nakanishi Y, Yin L (2018) Ultrasonic assisted high rotational speed diamond machining of dental glass ceramics. Int J Adv Manuf Technol:1–13
153. Lee W-c, Wei C-c, Chung S-C (2014) Development of a hybrid rapid prototyping system using low-cost fused deposition modeling and five-axis machining. J Mater Process Technol 214:2366–2374
154. Yamazaki T (2016) Development of a hybrid multi-tasking machine tool: integration of additive manufacturing technology with CNC machining. Procedia CIRP 42:81–86
155. Du W, Bai Q, Zhang B (2016) A novel method for additive/subtractive hybrid manufacturing of metallic parts. Procedia Manuf 5:1018–1030
156. Flynn JM, Shokrani A, Newman ST, Dhokia V (2016) Hybrid additive and subtractive machine tools—research and industrial developments. Int J Mach Tools Manuf 101:79–101